Oxidative Metabolism of Ferrocene Analogues of Tamoxifen: Characterization and Antiproliferative Activities of the Metabolites

Marie-Aude Richard, Didier Hamels, Pascal Pigeon, Siden Top, Patrick M. Dansette, Hui Zhi Shirley Lee, Anne Vessières, Daniel Mansuy, Gérard Jaouen

Oxidative Metabolism of Ferrocene Analogues of Tamoxifen: Characterization and Antiproliferative Activities of the Metabolites

Marie-Aude Richard, [a, b, c] Didier Hamels, [a] Pascal Pigeon, [a, b, c] Siden Top,*[b, c] Patrick M. Dansette, [d] Hui Zhi Shirley Lee, [a, b, c] Anne Vessières, [b, c] Daniel Mansuy,*[d] and Gérard Jaouen *[a, b, c]

a PSL, Chimie ParisTech, 11 rue Pierre et Marie Curie, 75005 Paris (France) E-mail: gerard.jaouen@chimie-paristech.fr

b Sorbonne Universités, UPMC Univ. Paris 6, UMR 8232, IPCM 4 place Jussieu, 75005 Paris (France). E-mail : siden.top@upmc.fr

c CNRS, UMR 8232, IPCM, 75005 Paris (France)

d Laboratoire de Chimie et Biochimie Pharmacologiques et Toxicologiques UMR 8601 CNRS, Université Paris Descartes, PRES Paris Cité Sorbonne 45 rue des Saints Pères, 75270, Paris Cedex 06 (France). E-mail: Daniel.Mansuy@parisdescartes.fr

Keywords: breast cancer, ferrocifen, indene metabolites, P450-dependent oxidation, quinone methides

Ferrociphenols have been found to have high antiproliferative activity against estrogen-independent breast cancer cells. The rat and human liver microsome-mediated metabolism of three compounds of the ferrocifen (**FC**) family, 1,1-bis(4-hydroxy-phenyl)-2-ferrocenyl-but-1-ene (**FC1**), 1-(4-hydroxyphenyl)-1-(phenyl)-2-ferrocenyl-but-1-ene (**FC2**), and 1-[4-(3-dimethylaminopropoxy)phenyl]-1-(4-hydroxyphenyl)-2-ferrocenyl-but-1-ene (**FC3**), was studied. Three main metabolite classes were identified: quinone methides (**QMs**) deriving from two-electron oxidation of **FCs**, cyclic indene products (**CPs**) deriving from acid-catalyzed cyclization of **QMs**, and allylic alcohols (**AAs**) deriving from hydroxylation of **FCs**. These metabolites are generated by cytochromes P450 (P450s), as shown by experiments with

either *N*-benzylimidazole as a P450 inhibitor or recombinant human P450s. Such P450-dependent oxidation of the phenol function and hydroxylation of the allylic CH_2 group of **FCs** leads to the formation of **QM** and **AA** metabolites, respectively. Some of the new ferrociphenols obtained in this study were found to exhibit remarkable antiproliferative effects toward MDA-MB-231 hormone-independent breast cancer cells.

Introduction

Bioorganometallic chemistry is a field of research that encompasses organometallic compounds in biology and medicine. Following the initial appearance of this term in 1985,[1] this field gradually became a hotbed of research into new applications of organometallics, particularly in therapy and diagnostics.[2-12] We have shown that some ferrocene derivatives are very active against cancer cells. The addition of a ferrocenyl moiety to selected polyaromatic phenols,[13-16] amines,[17,18] amides,[19] and esters[19,20] can potentiate their antiproliferative effects against breast and prostate cancer cells. For example, 4-hydroxytamoxifen, the active metabolite of the breast cancer drug tamoxifen,[21] shows limited cytotoxicity against hormone-refractory breast cancer cells (LC_{50} for MDA-MB-231 cells: 29 μM).[22] However, the ferrociphenol **FC3** (Figure 1), resulting from replacement of a phenyl group of hydroxytamoxifen with a ferrocenyl moiety, displays a dramatic improvement in cytotoxicity toward MDA-MB-231 cells (IC_{50} = 0.5μM).[14] Ferrociphenols (**FCs**, Figure 1) are easily oxidized at relatively low redox potentials, with formation of the corresponding quinone methides (**QMs**, Figure 1),[23,24] and it was recently shown that these reactive compounds are formed as a result of **FC** metabolism by liver microsomes,[25] and could play a role in the antitumor properties of **FCs**.[26]

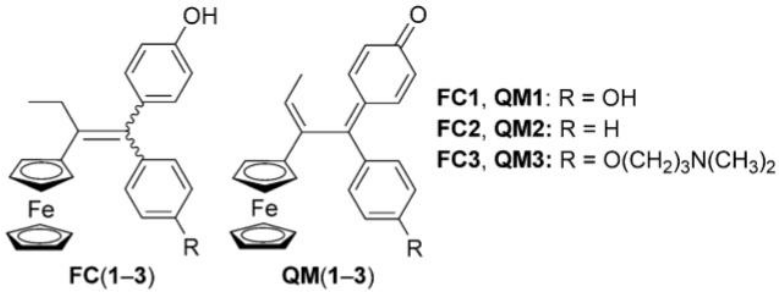

Figure 1. Ferrociphenols used as substrates in this study and their corresponding quinone methides (wavy-line bonds indicate the presence of both *cis* and *trans* isomers at the level of the double bond).

The aim of the work described herein was to study the metabolism of **FCs** by liver microsomes to determine whether some metabolites are cytotoxic toward MDA-MB-231 breast cancer cells, and, in a more general manner, to potentially find new molecules that are cytotoxic toward hormone-independent breast cancer cells. This article describes a study of the metabolism of three ferrociphenols **FC(1–3)** by liver microsomes, a characterization of their metabolites, and a comparison between the cytotoxicities of these metabolites against breast cancer cells and those of the parent compounds. Three main classes of metabolites are formed: 1) the corresponding quinone methides **QM(1–3)** as described above, 2) allylic alcohols derived from hydroxylation of the ferrociphenols at the allylic position, and 3) indene derivatives that result from an intramolecular cyclization of the quinone methides. Some of the new **FCs** obtained in this study show remarkable cytotoxic effects— even greater than those of their parent compounds—toward hormone-independent breast cancer cells.

Results and Discussion

Microsomal oxidation of FC1

An HPLC–MS study of incubations of **FC1** at 200 μM with liver microsomes from phenobarbital-pretreated rats in the presence of an NADPH-generating system for 30 min (conditions given in the Experimental Section below) showed the formation of three main metabolites in equivalent amounts. Those metabolites were not formed under identical incubations in the absence of NADPH. One of them exhibited UV/Vis (λ_{max} = 414 nm) and MS (molecular ion at m/z = 423) characteristics identical to those previously reported for the quinone methide **QM1** resulting from a two-electron oxidation of **FC1** (Table 1).[25]

The second metabolite exhibited a UV/Vis spectrum similar to that of **FC1** (λ_{max} = 237 with a shoulder at 290 nm, Figure 2 A and Table 1) and MS characteristics (molecular ion at m/z = 440) corresponding to a hydroxylated metabolite of **FC1**. Its tandem MS (MS^2) spectrum (Figure 2 B) showed major fragments at m/z = 422 ([*M*-18]) and 242 that should correspond to the loss of H_2O and a C(*para*-OH-C_6H_4)$_2$ fragment resulting from cleavage of the C=C bond, respectively. It also showed a fragment at m/z = 186 that was present in the MS^2 spectra of **FC1** and its three metabolites, and that corresponds to the ferrocene moiety. This metabolite was identified as an alcohol resulting from a hydroxylation of **FC1** on its ethyl moiety. This would lead to two possible alcohols, deriving either from an allylic hydroxylation or from a hydroxylation of the methyl group of **FC1**.

Table 1. MS, MS^2, and UV/Vis properties of the three common classes of ferrociphenol metabolites.

	M_r [Da] [a]	m/z		λ_{max} [nm] UV/Vis [d]
		MS [b]	MS^2 [c]	
FC1	424	424 $[M]^+$	422, 406, 394	240 (293)
QM1	422	423 $[M+H]^+$	357, 329, 186	414
CP1	422	422 $[M]^+$	407, 356, 186	323
AA1	440	440 $[M]^+$	422, 374, 242, 186	237 (290)
FC2	408	408 $[M]^+$	406, 379, 267	240 (292)
QM2	406	407 $[M+H]^+$	341, 313, 186	359
CP2	406	406 $[M]^+$	391, 340, 186	318
AA2	424	424 $[M]^+$	406, 242, 186	ND[e]
FC3	509	510 $[M+H]^+$	444, 424, 324	245 (297)
QM3	507	508 $[M+H]^+$	422, 329, 186	405
CP3	507	508 $[M+H]^+$	442, 329, 186	323
AA3	525	526 $[M+H]^+$	508, 422, 242	232 (287)

a Calculated molecular mass. b Molecular ion of MS spectra (ESI^+). c Main MS^2 fragments at 35 eV. d λ_{max} value of the spectra observed in HPLC–UV/Vis (see Experimental Section); for some compounds a clear shoulder was observed, the position of which is indicated in parentheses. [e] Not determined.

We tried to synthesize authentic samples of those two alcohols (Figure 3). Unfortunately, our attempts to obtain **AA1** failed. Only the primary alcohol **PA1** was obtained from reduction of the related ethyl ester **EE**[27] by lithium aluminum hydride (Scheme 1). The structure of **PA1** was determined by X-ray crystallographic analysis. Figure 4 shows the ORTEP diagram of the structure of **PA1**; crystallographic data are given in the Supporting Information, and selected bond distances and bond angles are summarized in the figure legend. The structure shows that the ferrocenyl group is oriented as far as possible from the aryl ring, thus avoiding potential steric clash with this group.

The retention time and spectral characteristics of **PA1** were clearly different from those of the alcohol metabolite, suggesting this metabolite to be the allylic alcohol **AA1** (Figure 3). This is in agreement with the much greater reactivity that should be expected for

the allylic position of **FC1** toward metabolic oxidation, and with the fact that one of the metabolites resulting from microsomal oxidation of tamoxifen is an allylic alcohol.[21, 28-32]

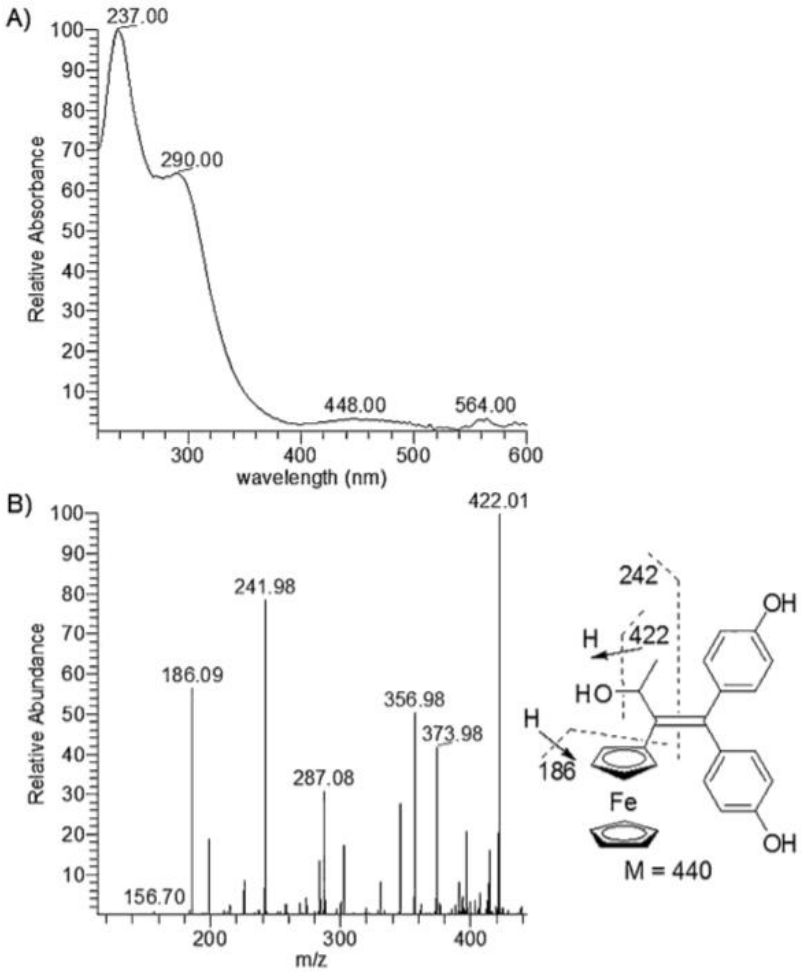

Figure 2. A) UV/Vis and B) MS^2 spectra of the second metabolite of **FC1**.

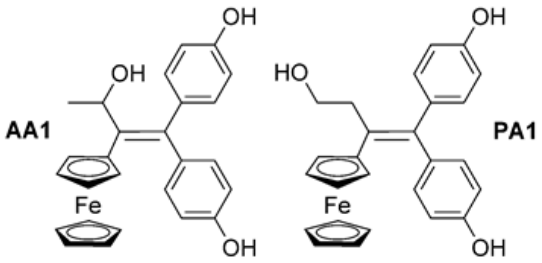

Figure 3. Alcohols **AA1** and **PA1** possibly deriving from hydroxylation of **FC1**.

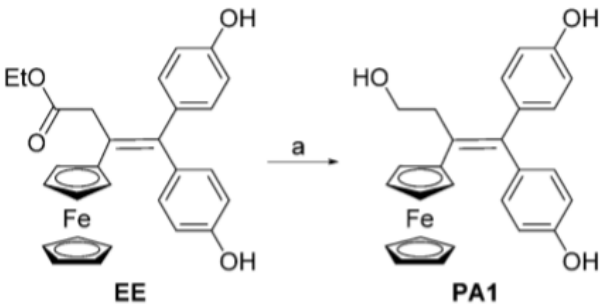

Scheme 1. Synthesis of primary alcohol **PA1**. *Reagents and conditions*: a) $LiAlH_4$, Et_2O, RT, 3 h, then reflux, 2 days, 71 %.

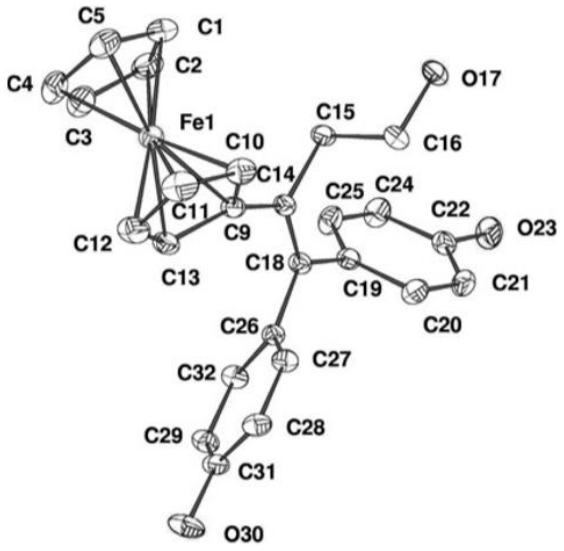

Figure 4. Molecular structure of **PA1**. Thermal ellipsoids are shown at 50 % probability. Selected bond distances [Å] and bond angles [°]: C(14)–C(18) 1.3350(15), C(14)–C(9) 1.4771(15), C(14)–C(15) 1.5184(15), C(18)–C(19) 1.4961(15), C(18)–C(26) 1.4885(15), C(9)–C(10) 1.4371(17), C(1)–C(2) 1.421(2), Fe(1)–C(9) 2.0601(11), Fe(1)–C(1) 2.0416(14); C(9)-C(14)-C(18) 122.33(10), C(14)-C(18)-C(26) 121.26(10), C(9)-C(14)-C(15) 116.02(10), C(19)-C(18)-C(26) 117.30(9).

The third metabolite of **FC1** exhibited a UV/Vis spectrum quite different from those of **FC1** and of the two other metabolites, with λ_{max} at 323 nm (Figure 5 A and Table 1). It was found to be formed when an authentic sample of **QM1** was submitted to a protic medium (H_2O or acetic acid used in the HPLC–MS studies). Indeed, this is described in the following section, as such an acid-catalyzed transformation was generally observed with all the quinone methides that we have previously obtained by oxidation of ferrociphenols.[25]

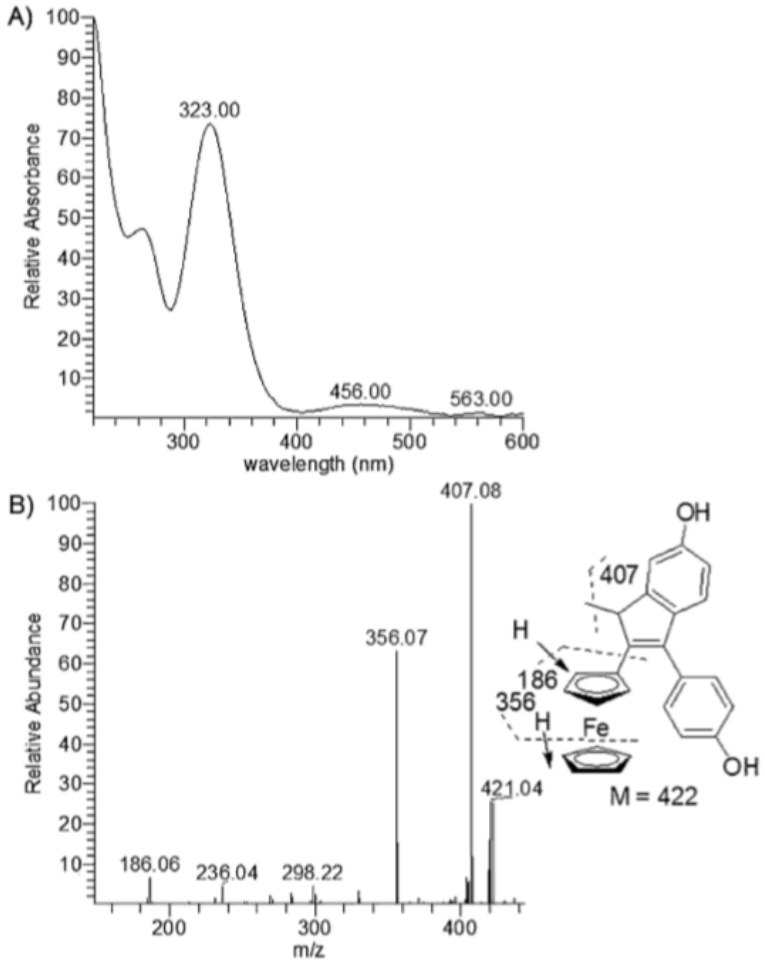

Figure 5. A) UV/Vis and B) MS^2 spectra of the third metabolite of **FC1**.

Acid-catalyzed cyclization of ferrociphenols to indene derivatives

In the presence of H_2O or acetic acid, quinone methides **QM1**, **QM2**, and **QM3** (Figure 1) were progressively transformed into compounds exhibiting λ_{max} ~ 320 nm (Table 1). Upon reaction of solutions of these quinone methides in dichloromethane with 3 equivalents of zinc(II) chloride, their conversion into cyclic compounds **CP1**, **CP2**, and **CP3** was complete (Scheme 2). These cyclized products, **CP**, should derive from a protonation of the oxygen atom of the quinone methide function followed by an electrophilic attack of the resulting allylic cation on the phenol ring, as shown in Scheme 2. The formation of such indene products from the cyclization of an allylic cation derived from the allylic alcohol of tamoxifen was previously reported.[33] This type of indene was also observed in the ruthenocifen series,[34] analogues of the ferrocifen series.

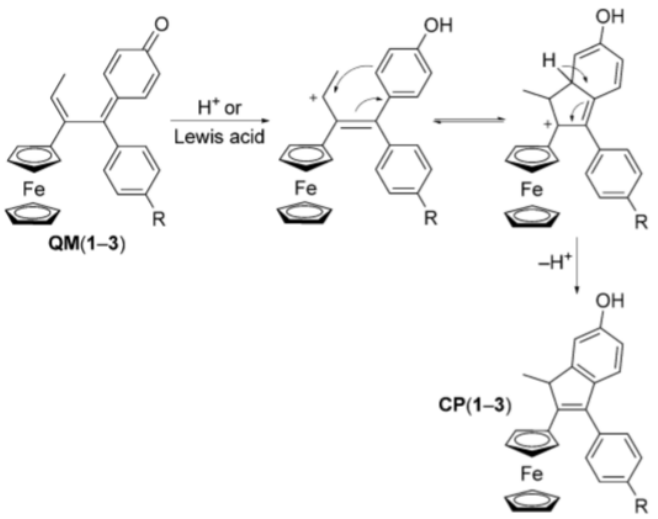

Scheme 2. Formation of indene compounds **CP(1–3)** from the acid-catalyzed cyclization of **QM(1–3)**.

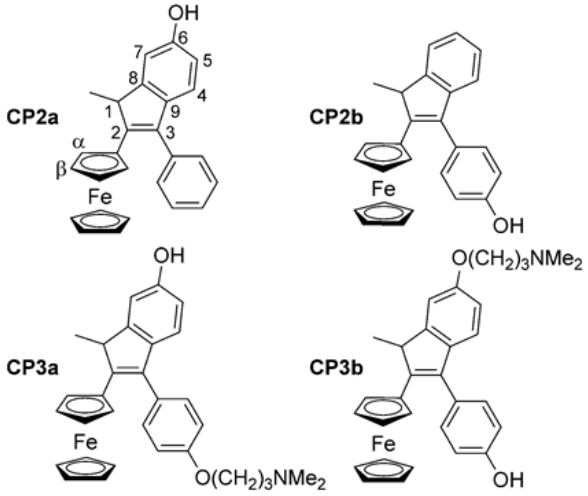

Figure 6. Possible isomers of cyclic compounds **CP2** and **CP3**.

In ^{1}H NMR spectra, these cyclic compounds are characterized by the presence of a doublet at ~ 1.50 ppm corresponding to their methyl group and a quadruplet at ~ 3.70 ppm corresponding to the CH group of their C5 ring. In the case of **CP2** and **CP3**, two isomers could be formed with respect to the two different arene rings on the molecule (Figure 6). However, acid-catalyzed cyclization of **QM2** only led to isomer **CP2a** in 74 % yield. Attachment of the $CHCH_3$ group to the phenol ring was confirmed by HMBC NMR experiments, which showed coupling signals between H1/C8, and CH_3/C8. Other ^{1}H and ^{13}C NMR, MS, and UV/Vis characteristics were in complete agreement with the indene structure. In the case of **CP3**, the two isomers **CP3a** and **CP3b** were isolated in 64 % yield

at a ratio of 7:3. The structure of the major isomer **CP3a** was identified by considering that its ^{1}H and ^{13}C NMR chemical shift values are closer to those of **CP2a** than those of **CP3b**. Table 2 lists selected ^{1}H and ^{13}C characteristics of **QMs** and **CPs**.

Table 2. Selected ^{1}H and ^{13}C NMR chemical shifts (δ [ppm]) of **CP** and **QM** metabolites in CD_3COCD_3.

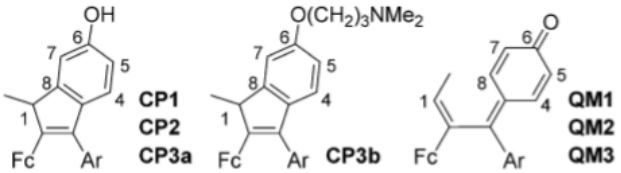

	Me	H1	H7	H4	H5	C7	C4	C5	C6
CP1	1.54	3.70	6.69	6.66	6.95	111.2	120.5	114.0	156.4
CP2	1.57	3.75	6.65	6.65	6.97	111.3	120.4	114.1	156.6
CP3a	1.55	3.72	6.67	6.66	6.95	111.3	120.4	114.1	156.5
CP3b	1.57	3.74	6.96	6.74	7.06	110.7	120.3	113.2	158.5
QM1[a]	1.61[b]	6.42[b]	–	–	–	–	–	–	–
QM2	1.70	6.45	6.35 or 6.39	7.49	6.35 or 6.39	–	–	–	186.8
QM3	1.65	6.44	6.34 or 6.36	7.55 or 7.60	6.34 or 6.36	–	–	–	186.8

a Determined in CD_3CN. b Only Me and H1 signals were clearly observed, whereas the aromatic ring signals were not well defined.

Interestingly, in the context of the following metabolic studies, some spectral characteristics allowed us to easily distinguish **QM** and **CP** metabolites (Tables 1 and 2). The UV/Vis spectra of the latter are significantly blue-shifted relative to the former (λ_{max} ~ 320 instead of ~ 400 nm). The MS molecular ion of the former corresponds to $[M + H]^+$, presumably due to protonation of the quinone oxygen atom, whereas that of the latter corresponds to $[M]^+$ (except in the case of **CP3**), probably resulting from a one-electron oxidation of the iron under the MS conditions (ESI^+). Finally, the MS^2 spectra of most **CP**

metabolites exhibited a major fragment at [*M*-15], corresponding to the loss of a methyl residue, as expected for their methyl-indene structure, which was not the case for **QM** metabolites. On the basis of the above data, the spectral characteristics of the third microsomal metabolite of **FC1** (Table 1) are in good agreement with the **CP1** structure.

Microsomal oxidation of FC2

An HPLC–MS study of microsomal incubations of **FC2** under conditions identical to those used for **FC1** showed the formation of three main metabolites. The major metabolite (~ 50 % of total metabolites) exhibited an HPLC retention time and spectral characteristics (λ_{max} = 318 nm, molecular ion at *m*/*z* = 406, and a major MS^2 fragment at *m*/*z* = 391; Table 1) identical to those of an authentic sample of **CP2** prepared, as described above, by treatment of **QM2** by $ZnCl_2$.

Another metabolite (~ 40 % of total metabolites) exhibited a molecular ion at *m*/*z* = 424 ([*M* + 16] relative to **FC2**) and MS^2 characteristics similar to those of **AA1** (major fragment corresponding to the loss of H_2O, presence of a fragment at *m*/*z* = 242 resulting from loss of the C(*para*-OH-C_6H_4)(C_6H_5) moiety after cleavage of the C=C bond, and a fragment at *m*/*z* = 186 corresponding to the ferrocene moiety; Table 1 and Figure 7). These data are in agreement with the allylic alcohol structure **AA2** shown in Figure 7 A.

The minor metabolite (~ 10 % of total metabolites) was more polar and also characterized by a molecular ion at *m*/*z* = 424 and a first fragment at *m*/*z* = 406 (loss of H_2O). Its MS^2 spectrum showed a fragment at *m*/*z* = 242 resulting from the loss of the C(*para*-OH-C_6H_4)(C_6H_5) moiety after cleavage of the C=C bond and a fragment at *m*/*z* = 186 corresponding to the ferrocene moiety. These data suggest that the hydroxylation occurred on the ethyl group of **FC2**. It also showed a fragment at *m*/*z* = 271 that could result from the loss of iron–cyclopentadienyl (FeCp) and a CH_2OH moiety (Figure 7 B). These data suggest that this minor metabolite could be the alcohol **PA2** resulting from hydroxylation of the **FC2** methyl group.

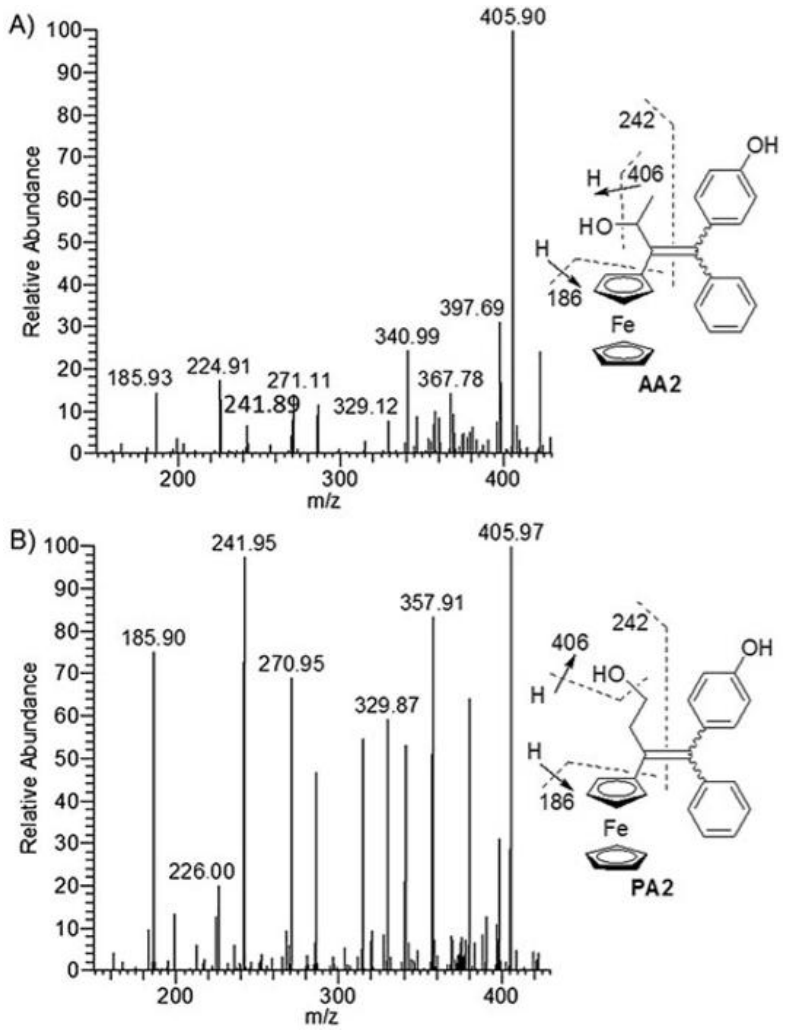

Figure 7. MS^2 spectra of the hydroxylated metabolites of **FC2**: A) **AA2** and B) **PA2**.

Notably, quinone methide **QM2** was only detected as a very minor product in microsomal incubations of **FC2**. In fact, HPLC–MS studies of **QM2** solutions in CH_3CN/H_2O mixtures showed its almost complete transformation into **CP2**.

Microsomal oxidation of FC3

Microsomal incubation of **FC3** under conditions identical to those used for **FC1** and **FC2** led to five main metabolites (Scheme 3). Three of them were derived from reactions that were previously observed for **FC1** and **FC2**: **QM3** and **CP3** (**a** and **b**) (Table 1) that were completely characterized by comparison of their HPLC retention times and UV/Vis and MS characteristics with those of authentic samples (**QM3** was described previously[25] and **CP3** was prepared as shown in Scheme 2), and a compound which could be the allylic alcohol

AA3. Its MS molecular ion at m/z = 526, corresponding to $[M + H]^+$ because of the protonation of the amine function, was expected for a metabolite of **FC3** having incorporated an oxygen atom (Table 1). Its UV/Vis spectrum (λ_{max} = 232 nm with a shoulder at 287 nm, Table 1) was similar to that previously observed for allylic alcohol **AA1**. Its MS^2 spectrum showed a major fragment at m/z = 508 (loss of H_2O) and a minor fragment at m/z = 242 that could result from the loss of the C(*para*-OH-C_6H_4)(*para*-R-C_6H_4) moiety after cleavage of the C=C bond. These data are in favor of structure **AA3** for this metabolite. This structure is very likely if one compares these data to those obtained above for microsomal metabolism of **FC1** and **FC2**, and because of the great reactivity of the allylic positions of **FC** derivatives.

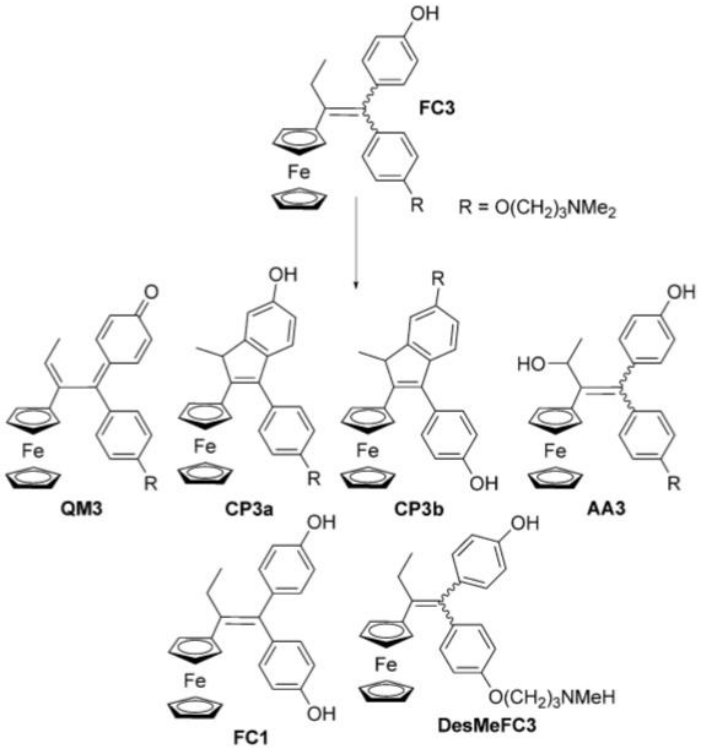

Scheme 3. Metabolites resulting from microsomal oxidation of **FC3**.

Two other metabolites were found to derive from oxidations occurring at the level of the **FC3** aminoalkyl chain. The major one had an HPLC retention time and MS and MS^2 characteristics identical to those of **FC1**. It should derive from hydroxylation of the CH_2 group of the aminoalkyl chain in the α position to the ether oxygen atom, which results in the loss of this chain. The mass spectrum of the second metabolite showed a molecular ion corresponding to $[M + H]^+$ at m/z = 496. This loss of 14 amu relative to **FC3** (m/z = 510) could be due to an oxidative demethylation of the $N(CH_3)_2$ function. This demethylated amino

compound was synthesized via the reaction sequence shown in Scheme 4.

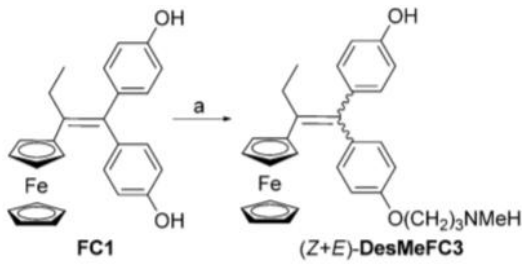

Scheme 4. Synthesis of **DesMeFC3**. *Reagents and conditions*: a) NaH, DMF, RT, 10 min, then $Cl(CH_2)_3NHCH_3 \cdot HCl$, 80 °C, overnight, 35 %.

The retention time and MS and MS^2 spectra of **DesMeFC3** were identical to those of the metabolite.

Compounds **FC2** and **FC3** are present as a mixture of two stereoisomers with *Z* or *E* configuration at the double bond.[15] Thus, their HPLC chromatogram exhibited two peaks of nearly equal intensity. Some of their microsomal metabolites, such as **AA2**, **AA3**, and **DesMeFC3**, also exhibited two more or less well-separated peaks that should correspond to their *Z* and *E* stereoisomers.

Oxidation of FC1 by human liver microsomes and recombinant human P450s

Incubations of **FC1**, **FC2**, and **FC3** with human liver microsomes under identical conditions led to very similar results with the formation of the same major metabolites. As all the metabolites described above derived from oxidation reactions that were almost completely inhibited by *N*-benzylimidazole, a typical inhibitor of cytochromes P450,[35] we also studied the ability of human recombinant P450s to catalyze these reactions. Experiments with commercially available microsomes of insect cells expressing P450 1A2, 2A6, 2B6, 2C8, 2C9, 2C19, 2D6, 2E1, and 3A4 showed P450s 2B6 and 3A4 to be the most active for the oxidation of **FC1** into **QM1**, **CP1**, and **AA1**, with an activity of 8.5 (2B6) and 6.6 (3A4) nmol (**QM1** + **CP1**) per nmol P450 per min, and 1.8 (2B6) and 2.2 (3A4) nmol **AA1** per nmol P450 per min.

Comparison of the antiproliferative properties of ferrociphenols and their metabolites

Ferrociphenols **FC1**, **FC2**, and **FC3** show strong antiproliferative effects on hormone-independent breast cancer cells (MDA-MB-231) with IC_{50} values ~ 1 µM.[14, 16, 19] Table 3 compares the IC_{50} values measured for these **FCs** with those of their microsomal metabolites, taking into account that **QM1** was too chemically unstable and that metabolites **AA1**, **AA2**, and **AA3** were obtained in quantities insufficient to permit the determination of IC_{50} values.

Table 3. Comparison of the antiproliferative effects of **FCs**, some of their microsomal metabolites, and **PA1**, toward hormone-independent breast cancer cells (MDA-MB-231).

Compd	IC_{50} [µM] [a]	Compd	IC_{50} [µM] [a]
FC1	0.6 ± 0.1[16]	**FC3**	0.5[14]
CP1	5.3 ± 0.4	**QM3**	1.8 ± 0.2
FC2	1.5 ± 0.1[19]	**CP3a**	2.7 ± 0.1
QM2	7.2 ± 0.5	**CP3b**	2.1 ± 0.2
CP2	17.2 ± 0.3	**DesMeFC3**	0.4 ± 0.1
		PA1	0.2 ± 0.1

a Values are the mean ± SD of two independent experiments.

The antiproliferative activities of freshly synthesized **QMs** were lower than those of their parent compounds; however, they are quite remarkable if one takes into account their high reactivity in the medium used for measurement of their antiproliferative activity, and the presumably small amounts that could reach the important cell target(s) in our assay conditions. Their contribution to the antiproliferative effects of **FCs** should be more pronounced in vivo, as they should be produced inside the cell, in the endoplasmic reticulum, close to the key cell targets.

The **CP** metabolites, which are much more stable in the medium, exhibited lower activities, with IC_{50} values 4- to 11- fold higher than that of the parent compound (Table 3). This suggests that they would not play a major role in the antiproliferative properties of the corresponding ferrociphenols. Interestingly, primary alcohol **PA1**, which was obtained by synthesis, was even more active than **FC1**, with a remarkable IC_{50} value of 0.2 µM. Because of their structural similarity, **AA1** and **PA1** could exhibit similar IC_{50} values. Thus, **AA1** and

the other allylic alcohol metabolites, **AA2** and **AA3**, might play a role in the antiproliferative effects of **FC**(**1**–**3**).

Conclusions

Three main classes of metabolites have been found in the microsomal oxidation of ferrociphenols **FC1**, **FC2**, and **FC3**: 1) quinone methides **QM** derived from two-electron oxidation of **FCs**, 2) indene products **CPs** derived from acid-catalyzed cyclization of **QMs**, and 3) allylic alcohols **AAs** derived from hydroxylation of **FCs** (Scheme 5). Their formation should be catalyzed by P450s, as shown by experiments using *N*-benzylimidazole or recombinant human P450s. Such P450-dependent oxidation of the phenol function and hydroxylation of the allylic CH_2 group of **FCs** respectively led to **QM** and **AA** metabolites. However, **QMs** were found to undergo an acid-catalyzed cyclization to indene derivatives **CPs** under the incubation conditions. This reaction was almost complete in the case of **FC2**, partial for **FC1**, and quite minor in the case of **FC3**. Formation of a quinone methide and an allylic alcohol similar to **QMs** and **AAs** in the metabolism of tamoxifen has been reported.[28-33, 36-38]

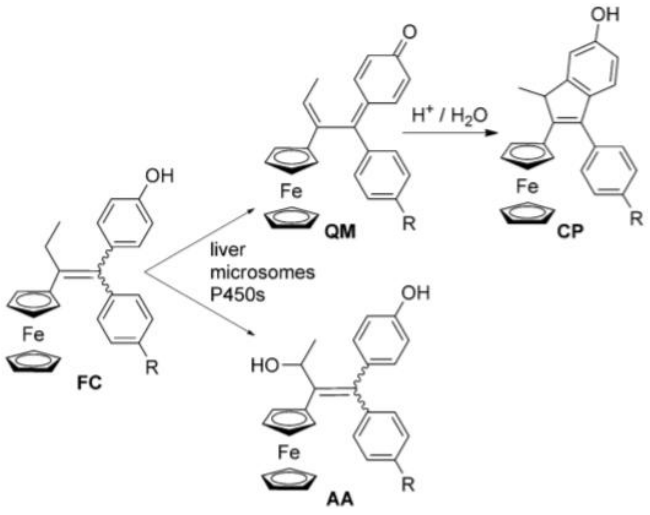

Scheme 5. Main metabolites formed upon oxidation of **FCs** by liver microsomes.

Ten of those **FC** metabolites were synthesized, and their cytotoxic activities toward hormone-independent breast cancer cells were compared with those of the parent compounds. All of them exhibited antiproliferative activities with IC_{50} values between 0.4 and 17 μM.

Some of the new compounds such as **DesMeFC3** and **PA1** exhibited IC_{50} values lower than those of **FCs**. **QM** and **CP** exhibit significant antiproliferative effects against hormone-independent breast cancer cells (MDA-MB-231), even if these values are one order of magnitude higher than those of **FCs** (Table 3). In fact, the IC_{50} value of **QM3** (1.8 μM) is only three- to fourfold greater than that of **FC3**. This should be related to the presumably very low amounts of **QM3** able to penetrate into the cell and to reach important cell targets in the assay used to measure its cytotoxic activity, given its much greater chemical reactivity than that of **FC3**. Considering that P450s are present in cancer cells,[39,40] it seems likely that because of their recently reported[26] effects on breast cancer cells, **QMs** could contribute to the cytotoxic effects of **FCs**. Our study has led to new compounds such as **DesMeFC3** and **PA1** that are even more active than **FCs**.

Experimental Section

All reagents and solvents were obtained from commercial suppliers. CH_2Cl_2 was distilled from P_2O_5 under argon. Acetone was dried over 4 Å molecular sieves. Thin-layer chromatography (TLC) was performed on silica gel 60 GF_{254}. Column chromatography was performed on Merck silica gel 60 (40–63 μm). Semi-preparative HPLC purification was undertaken with a Nucleodur column (5 μm, l = 25 cm, ∅ = 2.1 cm) using CH_3CN + (1 % Et_3N) as mobile phase. All NMR experiments [^1H, ^{13}C, and heteronuclear multiple bond correlation (HMBC)] were carried out at room temperature on Bruker 300 and 400 NMR spectrometers, and chemical shifts (δ) are reported in ppm relative to solvent residual peak; s, d, t and q are used to denote singlet, doublet, triplet, and quartet, respectively. UV/visible spectra were recorded on an Uvikon 942 spectrometer (Kontron Biotech) in CH_3OH or were obtained from the PDA detector of the HPLC system in elution mixtures of H_2O/CH_3CN 1% HCOOH. Mass spectrometry (MS) data were obtained on a Focus/ DSQII spectrometer for both electron impact (EI) and chemical ionization (CI) methods, and on an API 3000 PE Sciex Applied Biosystems spectrometer for the electrospray ionization (ESI) method. Elemental analyses were performed by the Laboratory of Microanalysis at ICSN of CNRS at Gif sur Yvette, France. Ferrociphenols **FC1**, **FC2**, and **FC3**,[15] and quinone methides, **QM2** and **QM3**,[25] were prepared by previously described procedures. All other products including enzymes were obtained from Sigma–Aldrich (St. Quentin Fallavier, France).

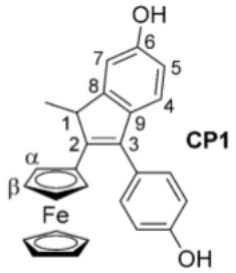

2-Ferrocenyl-1-methyl-3-(*p*-hydroxyphenyl)-1*H*-inden-6-ol (CP1): FC1 (0.280 g, 0.66 mmol) was dissolved in acetone (4 mL). Ag_2O (0.459 g, 1.98 mmol) was added in one portion as a solid. The mixture was stirred for 10 min at 40°C. The black solid, including the remaining Ag_2O, was eliminated by centrifugation (r.t., 5 min, 4000 *g*). $ZnCl_2$ (0.272 g, 2 mmol) was then added in one portion as a solid. The reaction was complete after 10 min of stirring. The mixture was then filtered over a 1 cm stick pad of silica gel. After solvent evaporation, the crude product was purified by silica gel column chromatography, using Et_2O/petroleum ether (PE) (2:1) as eluent. **CP1** was isolated as an orange solid (88 mg, 21 % yield): mp 88°C (dec.); ^{1}H NMR (300 MHz, CD_3COCD_3): δ=1.54 (d, J = 7.3 Hz, 3 H, Me), 3.70 (q, J = 7.3 Hz, 1 H, C*H*-Me), 4.02 (s, 5 H, Cp), 4.13–4.15 (m, 2 H, C_5H_4, $H_\alpha + H_\beta$), 4.17 (m, 1 H, C_5H_4, H_β), 4.28 (m, 1 H, C_5H_4, H_α), 6.66 (m, 1 H, C_6H_3, H4), 6.69 (m, 1 H, C_6H_3, H7), 6.95 (m, 1 H, C_6H_3, H5), 7.03 (d, J =8.6 Hz, 2 H, C_6H_4), 7.22 (d, J = 8.6 Hz, 2 H, C_6H_4), 8.15 (s, 1 H, OH), 8.54 ppm (s, 1 H, OH); ^{13}C NMR (75.46 MHz, CD_3COCD_3): δ = 20.4 (Me), 46.4 (C1), 67.2 (C_5H_4, C_α), 68.2 (C_5H_4, C_β), 69.1 (C_5H_4, C_β), 69.4 (C_5H_4, C_α), 70.0 (5 CH, Cp), 81.7 (C_5H_4, C*ip*), 111.2 (C_6H_3, C7), 114.0 (C_6H_3, C5), 116.4 (2CH, C_6H_4, C*m*), 120.5 (C_6H_3, C4), 129.1 (C_6H_4, C*ip*), 131.4 (2CH, C_6H_4, C*o*), 137.7 (C3), 139.5 (C_6H_4, C9), 143.5 (C2), 151.4 (C_6H_3, C8), 156.4 and 157.7 ppm (C6 and C*p*, 2 *C*-OH); MS (EI) *m*/*z*: 423.2 $[M+H]^+$; Anal. Calcd for $C_{26}H_{22}FeO_2 \cdot 0.5\,Et_2O + 0.5\,H_2O$: C 71.80, H 6.03, found: C 71.75, H 6.19. The presence of Et_2O and H_2O were detected in the NMR spectrum of **CP1**.

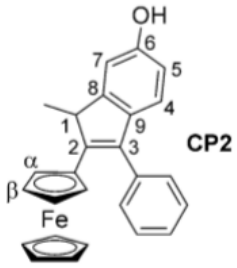

2-Ferrocenyl-1-methyl-3-phenyl-1*H*-inden-6-ol (CP2): QM2 (0.260 g, 0.64 mmol) was dissolved in CH_2Cl_2 (5 mL). $ZnCl_2$ (0.261 g, 1.92 mmol) was added in one portion as a solid. The mixture was stirred for 10 min. The mixture was then filtered over a 1 cm stick pad of silica gel. The compound was extracted from silica gel by washing with Et_2O (60 mL). After solvent evaporation, the crude product was purified by silica gel column chromatography using Et_2O/ PE (1:1) as eluent. **CP2** was isolated as an orange solid (193 mg, 74 % yield): mp 172 °C; ^{1}H NMR (300 MHz, CD_3COCD_3): δ=1.57 (d, *J* =7.3 Hz, 3 H, Me), 3.75 (q, *J* =7.3 Hz, 1 H, C*H*-Me), 4.03 (s, 5 H, Cp), 4.08 (m, 1 H, C_5H_4, H_α), 4.14 (m, 1 H, C_5H_4, H_β), 4.15 (m, 1 H, C_5H_4, H_β), 4.25 (m, 1 H, H, C_5H_4, H_α), 6.65 (m, 2 H, C_6H_3, H7 + H4), 6.97 (m, 1 H, C_6H_3, H5), 7.40 (d, *J* =7.5 Hz, 2 H, H*o*, C_6H_5), 7.47 (t, *J* =7.5 Hz, 1 H, H*p*, C_6H_5), 7.57 (t, *J* = 7.5 Hz, 2 H, H*m*, C_6H_5), 8.16 ppm (br s, 1 H, OH); ^{13}C NMR (75.46 MHz, CD_3COCD_3): δ=20.4 (Me), 46.6 (C1), 67.2 (C_5H_4, C_α), 69.0 (C_5H_4, C_β), 69.3 (C_5H_4, C_β), 69.4 (C_5H_4, C_α), 70.1 (5 CH, Cp), 81.4 (C_5H_4, C*ip*), 111.3 (C_6H_3, C7), 114.1 (C_6H_3, C5), 120.4 (C_6H_3, C4), 128.2 (C_6H_5, C*p*), 129.5 (C_6H_5, C*m*), 130.3 (C_6H_5, C*o*), 137.7 (C3), 138.5 (C_6H_5, C*ip*), 139.2 (C_6H_3, C9), 143.2 (C2), 151.5 (C_6H_3, C8), 156.6 ppm (C6, *C*-OH). HMBC experiments confirmed the indicated structure. MS (ESI) *m*/*z*: 406.2 $[M]^+$; Anal. calcd for $C_{26}H_{22}FeO$: C 76.86, H 5.46, found: C 76.43, H 5.50.

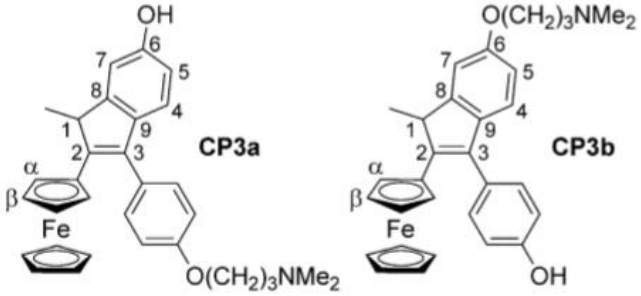

2-Ferrocenyl-1-methyl-3-(*p*-(3-(dimethylamino)propoxy)phenyl)-1*H*-inden-6-ol (CP3a) and 2-ferrocenyl-1-methyl-3-(*p*-hydroxy-phenyl)-6-(dimethylamino)propoxy)-1*H*-indene (CP3b): FC3 (0.255 g, 0.50 mmol) was dissolved in acetone (10 mL). Ag_2O (0.348 g, 1.5

mmol) was added in one portion as a solid. The mixture was stirred for 1.5 h. A black solid, including the remaining Ag_2O, was eliminated by centrifugation (r.t., 5 min, 4000 *g*) and the solution was evaporated. The obtained **QM3** was then dissolved in CH_2Cl_2 (10 mL). $ZnCl_2$ (0.272 g, 2 mmol) was added in one portion as a solid. The mixture was stirred for 45 min. Then, the mixture was filtered over a 1 cm stick pad of silica gel. The compound was extracted from silica gel by washing with acetone/Et3N (9:1). After solvent evaporation, the crude product was purified by short silica gel column, using acetone/Et3N (9:1) as eluent. A mixture (162 mg) of the two isomers of **CP3** were isolated (64 % yield). The two isomers were separated by semi-preparative HPLC (normal phase), using acetone/Et_3N (20:1) as eluent. The first isomer, **CP3a**, was obtained as an orange solid (75 mg): mp 135 °C; ^{1}H NMR (300 MHz, CD_3COCD_3): δ=1.55 (d, *J* = 7.3 Hz, 3 H, Me), 1.97 (m, 2 H, CH_2), 2.21 (s, 6 H, $N(CH_3)_2$), 2.47 (t, *J* = 7.1 Hz, 2 H, CH_2-N), 3.72 (q, *J* = 7.3 Hz, 1 H, *CH*-Me), 4.02 (s, 5 H, Cp), 4.10–4.17 (m, 5 H, OCH_2 + C_5H_4), 4.26–4.27 (m, 1 H, C_5H_4, H*o*), 6.66 (d, *J* = 2.0 Hz, 1 H, C_6H_3, H4), 6.67 (d, *J* =0.7 Hz, 1 H, C_6H_3, H7), 6.95 (m, 1 H, C_6H_3, H5), 7.11 (d, *J* = 8.8 Hz, 2 H, C_6H_4, H*m*), 7.30 (d, *J* = 8.8 Hz, 2 H, C_6H_4, H*o*), 7.96 ppm (s, 1 H, OH); ^{13}C NMR (75.46 MHz, CD_3COCD_3): δ=20.4 (CH_3), 28.3 (CH_2), 45.7 (NMe_2), 46.5 (CH, C1), 56.9 (CH_2-N), 66.8 (CH2, CH_2O), 67.2 (1 CH, C_5H_4), 68.9 (1 CH, C_5H_4), 69.2 (1 CH, C_5H_4), 69.4 (1 CH, C_5H_4), 70.0 (5 CH, Cp), 81.6 (C, C_5H_4, C*ip*), 111.3 (C_6H_3, C7), 114.1 (C_6H_3, C5), 115.4 (2 CH, C_6H_4, C*m*), 120.4 (C_6H_3, C4), 130.1 (C_6H_4, C*ip*), 131.3 (2 CH, C_6H_4, Co), 137.4 (C3), 139.4 (C9), 143.0 (C2), 151.4 (C8), 156.5 (C6), 159.5 ppm (C, C*p*); MS (CI) *m*/*z*: 508 $[M+H]^+$; Anal. calcd for $C_{31}H_{33}FeNO_2 \cdot 0.7\,H_2O$: C 71.59, H 6.67, N 2.69, found: C 71.65, H 6.76, N 2.40. The second isomer, **CP3b**, was obtained as an orange solid: mp 186 °C; ^{1}H NMR (300 MHz, CD_3COCD_3): δ=1.57 (d, *J* =7.3 Hz, 3 H, Me), 1.90 (m, 2 H, CH_2), 2.18 (s, 6 H, NMe_2), 2.42 (t, 2 H, *J* = 7.1 Hz, CH_2-N), 3.74 (q, *J* = 7.3 Hz, 1 H, *CH*-Me), 4.02 (s, 5 H, Cp), 4.05 (t, *J* = 6.4 Hz, 2 H, OCH_2), 4.14–4.19 (m, 3 H, C_5H_4), 4.29–4.30 (m, 1 H, C_5H_4, H*o*), 6.74 (d, *J* = 2.1 Hz, 1 H, C_6H_3, H4), 6.96 (d, *J* = 0.7 Hz, 1 H, C_6H_3, H7), 7.04 (d, *J* = 8.6 Hz, 2 H, C_6H_4, H*m*), 7.06 (m,1 H, C_6H_3, H5), 7.23 (d, *J* = 8.6 Hz, 2 H, C_6H_4, H*o*), 7.96 ppm (s, 1 H, OH); ^{13}C NMR (75.46 MHz, CD_3COCD_3): δ=20.4 (CH_3), 28.4 (CH_2), 45.7 (NMe_2), 46.5 (CH, C1), 56.9 (CH_2-N), 67.0 (CH_2, CH_2O), 67.3 (1 CH, C_5H_4), 68.9 (1 CH, C_5H_4), 69.2 (1 CH, C_5H_4), 69.5 (1 CH, C_5H_4), 70.0 (5 CH, Cp), 81.5 (C, C_5H_4, C*ip*), 110.7 (C_6H_3, C7), 113.2 (C_6H_3, C5), 116.4 (2 CH, C_6H_4, C*m*), 120.3 (C_6H_3, C4), 128.9 (C_6H_4, C*ip*), 131.4 (2 CH, C_6H_4, C*o*), 137.5 (C3), 140.5 (C9), 143.7 (C2), 151.3 (C8), 157.8 (C*p*), 158.5 ppm (C6); MS (CI) *m*/*z*: 508 $[M+H]^+$; Anal. calcd for $C_{31}H_{33}FeNO_2$: C 73.37, H 6.55, N, 2.76, found: C 73.60, H 6.60, N 2.98.

2-Ferrocenyl-1,1-bis-(4-hydroxyphenyl)-4-hydroxy-but-1-ene (PA1): To a stirred suspension of $LiAlH_4$ (0.787 g, 20.7 mmol, 4 equiv) in Et_2O (200 mL) at 0 °C was added dropwise a solution of ethyl-3-en-3-ferrocenyl-4,4-bis-(4-hydroxyphenyl) butanoate, **EE**, (2.5 g, 5.18 mmol) in THF (50 mL). The mixture was stirred at room temperature for 3 h, then at reflux for two days. After cooling to room temperature, EtOAc, followed by EtOH, were added dropwise. The mixture was poured into a saturated solution of $NaHCO_3$ and extracted with Et_2O (3x 300 mL). The combination of organic layers was washed with H_2O and dried over $MgSO_4$. After filtration and concentration under reduced pressure, the crude product was purified by semi-preparative HPLC using CH_3CN/H_2O (55:45) as eluent. 2-Ferrocenyl-1,1-bis-(4-hydroxyphenyl)-4-hydroxy-but-1-ene, **PA1**, was obtained in 71 % yield as an orange solid (2.28 g); ^{1}H NMR (300 MHz; CD_3COCD_3): δ=2.98–3.08 (m, 2 H, CH_2), 3.62–3.74 (m, 3 H, CH_2O+ OH), 4.08 (t, *J* = 1.9 Hz, 2 H, C_5H_4), 4.18 (t, *J* =1.9 Hz, 2 H, C_5H_4), 4.25 (s, 5 H, Cp), 6.80 (d, *J* =8.7 Hz, 2 H, C_6H_4), 6.93 (d, *J* =8.7 Hz, 2 H, C_6H_4), 6.96 (d, *J* =8.7 Hz, 2 H, C_6H_4), 7.18 (d, *J* =8.7 Hz, 2 H, C_6H_4), 8.33 (bs, 1 H, OH), 8.39 ppm (bs, 1 H, OH); ^{13}C NMR (75.46 MHz; CD_3COCD_3): δ=39.5 (CH_2), 62.9 (CH_2, CH_2O), 68.6 (2 CH, C_5H_4), 69.8 (5 CH, Cp), 70.1 (2 CH, C_5H_4), 88.8 (C, C_5H_4*ip*), 115.7 (2 CH, C_6H_4), 115.9 (2 CH, C_6H_4), 131.2 (2 CH, C_6H_4), 131.8 (2 CH, C_6H_4), 137.0 (C), 137.3 (C), 140.6 (C), 145.8 (C), 156.7 (C, C-OH), 156.8 ppm (C, C-OH); MS (EI, 70 eV) *m*/*z*: 440 $[M]^{+\cdot}$, 375 $[M\text{-Cp}]^+$, 121 $[FeCp]^+$; Anal. calcd for $C_{26}H_{24}FeO_3$: C 70.92, H 5.49, found: C 70.64, H 5.55.

2-Ferrocenyl-1-(4-hydroxyphenyl)-1-(4-(3-methylaminopropoxy)-phenyl)-but-1-ene (DesMeFC3): NaH (0.48 g, 12 mmol, 60 % purity) was slowly added to a solution of **FC1** (1.27 g, 3 mmol) dissolved in DMF (50 mL). After stirring for 10 min, *N*-methyl-3-chloro-propylamine hydrochloride (0.519 g, 3.6 mmol) was added, and the mixture was left to stir overnight at 80°C. After cooling to room temperature, EtOH (2 mL) was added to eliminate unreacted NaH. The mixture was then poured into a saturated $NaHCO_3$ solution and extracted with EtOAc (3 x 200 mL). The combination of organic layers was dried over $MgSO_4$. After concentration under reduced pressure, the crude product was subjected to silica gel column chromatography. The compounds were first eluted with acetone (to remove unreacted **FC1**), then with acetone/Et_3N (90:10). **DesMeFC3** was obtained as an orange oil in 35 % yield (0.52 g), as a mixture of *Z* and *E* isomers (50 :50); ^{1}H NMR (300 MHz, CD_3COCD_3): δ=1.00 (t, *J* =7.5 Hz, 3 H, Me, one isomer), 1.01 (t, *J* = 7.5 Hz, 3 H, Me, one isomer), 1.83–1.92 (m, 2 H, CH_2, both isomers), 2.34 (s, 3 H, N(CH_3), one isomer), 2.36 (s, 3 H, N(CH_3), one isomer), 2.58–2.64 (m, 2 H, CH_2, both isomers), 2.66–2.72 (m, 2 H, CH_2-N, both isomers), 3.89 (t, *J* =1.8 Hz,

2 H, C_5H_4, one isomer), 3.91 (t, J = 1.8 Hz, 2 H, C_5H_4, one isomer), 3.98–4.07 (m, 4 H, OCH_2 + C_5H_4, both isomers), 4.10 (s, 5 H, Cp, both isomers), 6.68–7.14 ppm (8d, 8 H, C_6H_4, both isomers); ^{13}C NMR (75.46 MHz, CD_3COCD_3): δ=15.9 (CH_3), 28.4 (CH_2), 29.4 (CH_2), 35.8 (NMe), 48.9 (CH_2), 66.6 (OCH_2), 68.7 (2 CH, C_5H_4), 69.7 (2 CH, C_5H_4), 69.9 (5 CH, Cp), 87.9 (C, C_5H_4, C*ip*), 114.9 (C_6H_4, one isomer), 115.0 (C_6H_4, one isomer), 131.1 (C_6H_4), 131.7 (C_6H_4), 136.8 (C), 137.1 (C), 138.4 (C), 138.5 (C), 156.8 (C), 158.4 ppm (C); MS (CI) *m*/*z*: 496 $[M + H]^+$; Anal. calcd for $C_{30}H_{33}FeNO_2 \cdot 0.5\,H_2O$: C 71.43, H 6.79, N 2.78, found: C 71.27, H 7.03, N 3.20.

X-ray crystal structure determinations for **PA1**: Data were recorded at 200 K on a Bruker APEX-II CCD diffractometer with graphite monochromated Mo*Ka* radiation (λ = 0.71073 Å) and the w and F scan technique. Data were corrected for Lorentz and polarization effects, and semi-empirical absorption correction based on symmetry equivalent reflections was applied by using the SADABS program.[41,42] Orientation matrix and lattice parameters were obtained by least-squares refinement of the diffraction data of 9821 reflections within the range 2° < θ < 30°. The structure was solved by direct methods and refined with full-matrix least-squares technique on F^2 using the CRYSTALS [43] program. All non-hydrogen atoms were refined anisotropically. All hydrogen atoms were either set in calculated positions and isotropically refined. $C_{26}H_{24}FeO_3$: M_r=440.32 Da; monoclinic $P21/c$; a = 9.9877(4), b = 20.7297(8), c =10.6135(4) Å; β = 108.554(10)°; V = 2083.23(14) Å^3; Z = 4. The data were collected in the *hkl* range: -14 to 13, -26 to 29, -12 to 15; total reflections collected: 32389; independent reflections: 6375. Data were collected up to a 2θ max value of 60°. Number of variables: 272; $R(I > 2\sigma(I))$ = 0.030, wR2(all) = 0.062, S = 1.00; highest residual electron density: 0.49 eÅ^3. CCDC-1031238 contains the supplementary crystallographic data for this paper. These data can be obtained free of charge from The Cambridge Crystallographic Data Centre via www.ccdc.cam.ac.uk/cgi-bin/catreq.cgi.

Incubations of FCs with liver microsomes: Microsomes (2 nmol P450 mg protein) were prepared from the livers of rats pretreated with phenobarbital (1 g per liter of drinking water for 7 days) as described previously.[44] Human liver microsomes and insect cell microsomes expressing recombinant human cytochromes P450 were obtained from BD-Gentest (Le Pont de Claix, France). Cytochrome P450 was assayed by the method of Omura and Sato.[45] Proteins were measured according to the method of Lowry et al. using bovine serum albumin as standard.[46] Typical incubations were performed in potassium phosphate buffer (0.1 m, pH 7.4)

containing microsomes (1–2 μM P450), 1 mm NADP, 15 mm glucose-6-phosphate, 2 U mL^{-1} glucose-6-phosphate dehydrogenase, and substrate (50–500 μM) at 37°C. Reactions were stopped either by adding one-half volume of CH_3CN/CH_3COOH (9:1) and centrifugation of precipitated proteins (12 000 *g*, 10 min) or by solid-phase extraction using Oasis columns (Waters, St. Quentin en Yvelines, France; 1 mL loading, 1 mL H_2O wash, and 1 mL CH_3OH elution), evaporation of the solvent with N_2, and re-dissolution in the HPLC mobile phase.

HPLC–MS analyses: HPLC–MS studies were performed on a Survey- or HPLC instrument coupled to an LCQ Advantage ion trap mass spectrometer (Thermo, Les Ulis, France), using a Biobasic C_{18} column (100 mm x2 mm, 3 μm) and a 20 min linear gradient of ammonium acetate (10 mm, pH 4.6) to B) $CH_3CN/CH_3OH/H_2O$ (7:2:1) mixture, at 200 μL min^{-1}. For some compounds an alternative gradient system was used: A) H_2O/HCOOH 0.1 % and B) CH_3CN/HCOOH 0.1 %. ESI-MS data were obtained in positive ionization mode detection under the following conditions: source parameters: sheath gas, 20; auxiliary gas, 5; spray voltage, 4.5 kV; capillary temperature, 200 °C; capillary voltage, 15 V; and *m*/*z* range for MS recorded generally between 200 and 760.

Cytotoxicity measurements: As previously reported,[16] stock solutions (1–10 mM) of the compounds to be tested were prepared in DMSO and were kept at -20 °C in the dark. Serial dilutions in Dulbecco's modified Eagle's medium (DMEM) without phenol red/Glutamax I were prepared just prior to use. DMEM without phenol red, Glutamax I and fetal bovine serum (FBS) were purchased from Gibco; MDA-MB-231 cells were obtained from the ATCC (Manassas, VA, USA). Cells were maintained in a monolayer culture in DMEM with phenol red/Glutamax I supplemented with 9% FBS at 37 °C in a 5 % CO_2/air humidified incubator. For proliferation assays, MDA-MB-231 cells were plated in 1 mL DMEM without phenol red, supplemented with 10 % de-complemented and hormone-depleted FBS, 1% kanamycin, 1% Glutamax I and incubated. The following day (day 0), 1 mL of the same medium containing the compounds to be tested was added to the plates. At day 3 the incubation medium was removed, and 2 mL of the fresh medium containing the compounds were added. After 5 days the total protein content of the plate was analyzed as follows: cell monolayers were fixed for 1 h at room temperature with methylene blue (1 mg mL^{-1} in 50:50 H_2O/CH_3OH), then washed with H_2O. After the addition of HCl (0.1 M, 2 mL), the plate was incubated for 1 h at 37 °C and then the absorbance of each well (four wells for each concentration) was

measured at λ 650 nm with a Bio-Rad spectrophotometer. The results are expressed as the percentage of proteins versus control.

Acknowledgements

The Agence Nationale de la Recherche (ANR-10-BLAN-706, Mecaferrol) is gratefully acknowledged for financial support. The authors acknowledge COST Actions CM1105 for financial support and for fostering fruitful discussions among authors, and Patrick Herson (Université Pierre et Marie Curie, Paris, IPCM and LabEx-Michem) for crystal structure determination.

[1] S. Top, G. Jaouen, A. Vessieres, J. P. Abjean, D. Davoust, C. A. Rodger, B. G. Sayer, M. J. McGlinchey, *Organometallics* **1985**, *4*, 2143–2150.

[2] *Bioorganometallics* (Ed.: G. Jaouen), Wiley-VCH, Weinheim, **2006**.

[3] C. G. Hartinger, N. Metzler-Nolte, P. J. Dyson, *Organometallics* **2012**, *31*, 5677–5685.

[4] N. P. E. Barry, P. J. Sadler, *Chem. Commun.* **2013**, *49*, 5106–5131.

[5] B. Bertrand, A. Casini, *Dalton Trans.* **2014**, *43*, 4209–4219.

[6] B. Biersack, R. Schobert, *Curr. Med. Chem.* **2009**, *16*, 2324–2337.

[7] S. S. Braga, A. M. S. Silva, *Organometallics* **2013**, *32*, 5626–5639.

[8] *Topics in Organometallic Chemistry: Medicinal Organometallic Chemistry*, *Vol. 32* (Eds.: G. Jaouen, N. Metzler-Nolte), Springer, Berlin, **2010**.

[9] D. Dive, C. Biot, *Curr. Top. Med. Chem.* **2014**, *14*, 1684–1692.

[10] R. Alberto, *J. Organomet. Chem.* **2007**, *692*, 1179–1186.

[11] N. Metzler-Nolte, M. Salmain in *Ferrocenes: Ligands, Materials and Biomolecules* (Ed.: Stepnicka), Wiley, Chichester, **2008**, pp. 499–639.

[12] G. Jaouen, S. Top in *Advances in Organometallic Chemistry and Catalysis*, The Silver/Gold Jubilee International Conference on Organometallic Chemistry Celebration Book (Ed.: A. J. L. Pombeiro), Wiley, Hoboken, **2014**, pp. 563–580.

[13] S. Top, J. Tang, A. Vessières, D. Carrez, C. Provot, G. Jaouen, *Chem. Commun.* **1996**, 955–956.

[14] A. Nguyen, A. Vessières, E. A. Hillard, S. Top, P. Pigeon, G. Jaouen, *Chimia* **2007**, *61*, 716–724.

[15] S. Top, A. Vessières, G. Leclercq, J. Quivy, J. Tang, J. Vaissermann, M. Huché, G. Jaouen, *Chem. Eur. J.* **2003**, *9*, 5223–5236.

[16] A. Vessières, S. Top, P. Pigeon, E. A. Hillard, L. Boubeker, D. Spera, G. Jaouen, *J. Med. Chem.* **2005**, *48*, 3937–3940.

[17] P. Pigeon, S. Top, O. Zekri, E. A. Hillard, A. Vessieres, M.-A. Plamont, O. Buriez, E. Labbe, M. Huché, S. Boutamine, C. Amatore, G. Jaouen, *J. Organomet. Chem.* **2009**, 694, 895–901.

[18] M. Görmen, P. Pigeon, S. Top, A. Vessières, M.-A. Plamont, E. A. Hillard, G. Jaouen, *MedChemComm* **2010**, *1*, 149–151.

[19] M. Görmen, P. Pigeon, S. Top, E. A. Hillard, M. Huché, C. G. Hartinger, F. de Montigny, M.-A. Plamont, A. Vessières, G. Jaouen, *ChemMedChem* **2010**, *5*, 2039–2050.

[20] J. B. Heilmann, E. A. Hillard, M.-A. Plamont, P. Pigeon, M. Bolte, G. Jaouen, A. Vessières, *J. Organomet. Chem.* **2008**, *693*, 1716–1722.

[21] B. Testa, S. D. Kramer, *Chem. Biodiversity* **2009**, *6*, 591–684.

[22] D. Yao, F. Zhang, L. Yu, Y. Yang, R. B. van Breemen, J. L. Bolton, *Chem. Res. Toxicol.* **2001**, *14*, 1643–1653.

[23] E. A. Hillard, A. Vessières, L. Thouin, G. Jaouen, C. Amatore, *Angew. Chem. Int. Ed.* **2006**, *45*, 285–290; *Angew. Chem.* 2006, *118*, 291–296.

[24] P. Messina, E. Labbé, O. Buriez, E. A. Hillard, A. Vessières, D. Hamels, S. Top, G. Jaouen, Y. M. Frapart, D. Mansuy, C. Amatore, *Chem. Eur. J.* **2012**, *18*, 6581–6587.

[25] D. Hamels, P. M. Dansette, E. A. Hillard, S. Top, A. Vessières, P. Herson, G. Jaouen, D. Mansuy, *Angew. Chem. Int. Ed.* **2009**, *48*, 9124 –9126; *Angew. Chem.* **2009**, *121*, 9288–9290.

[26] A. Citta, A. Folda, A. Bindoli, P. Pigeon, S. Top, A. Vessières, M. Salmain, G. Jaouen, M. P. Rigobello, *J. Med. Chem.* **2014**, *57*, 8849–8859.

[27] P. Pigeon, M. Görmen, K. Kowalski, H. Müller-Bunz, M. J. McGlinchey, S. Top, G. Jaouen, *Molecules* **2014**, *19*, 10350–10369.

[28] D. J. Boocock, J. L. Maggs, I. N. H. White, B. K. Park, *Carcinogenesis* **1999**, *20*, 153–160.

[29] S. Y. Kim, N. Suzuki, L. Y. R. Santosh, R. Rieger, S. Shibutani, *Chem. Res. Toxicol.* **2003**, *16*, 1138–1144.

[30] L. M. Notley, K. H. Crewe, P. J. Taylor, M. S. Lennard, E. M. J. Gillam, *Chem. Res. Toxicol.* **2005**, *18*, 1611–1618.

[31] L. M. Notley, W. C. J. F. De, R. M. Wunsch, R. G. Lancaster, E. M. J. Gillam, *Chem. Res. Toxicol.* **2002**, *15*, 614–622.

[32] T. S. Dowers, Z. H. Qin, G. R. J. Thatcher, J. L. Bolton, *Chem. Res. Toxicol.* **2006**, *19*, 1125–1137.

[33] C. Sanchez, R. A. McClelland, *Can. J. Chem.* **2000**, *78*, 1186–1193.

[34] H. Z. S. Lee, O. Buriez, E. Labbé, S. Top, P. Pigeon, G. Jaouen, C. Amatore, W. K. Leong, *Organometallics* **2014**, *33*, 4940–4946.

[35] M. A. Correia, P. R. Ortiz de Montellano in *Cytochrome P450 Structure, Mechanism, and Biochemistry, 3rd ed.* (Ed.: P. R. Ortiz de Montellano), Kluwer Academic/Plenum, New York, **2005**, pp. 247–295.

[36] P. W. Fan, F. Zhang, J. L. Bolton, *Chem. Res. Toxicol.* **2000**, *13*, 45–52.

[37] M. M. Marques, F. A. Beland, *Carcinogenesis* **1997**, *18*, 1949–1954.

[38] J. L. Bolton, *Curr. Org. Chem.* **2014**, *18*, 61–69.

[39] L. J. Yu, J. Matias, D. A. Scudiero, K. M. Hite, A. Monks, E. A. Sausville, D. J. Waxman, *Drug Metab. Dispos.* **2001**, *29*, 304–312.

[40] V. P. Androutsopoulos, K. Ruparelia, R. R. J. Arroo, A. M. Tsatsakis, D. A. Spandidos, *Toxicology* **2009**, *264*, 162–170.

[41] G. M. Sheldrick, *SADABS, Program for scaling and correction of area detector data*, **1997**, University of Göttingen, Germany.

[42] R. H. Blessing, *Acta Crystallogr. Sect. A* **1995**, *51*, 33–38.

[43] P. W. Betteridge, J. R. Carruthers, R. I. Cooper, K. Prout, D. J. Watkin, *J. Appl. Crystallogr.* **2003**, *36*, 1487–1487.

[44] P. Kremers, P. Beaune, T. Cresteil, J. De Graeve, S. Columelli, J. P. Leroux, J. E. Gielen, *Eur. J. Biochem.* **1981**, *118*, 599–606.

[45] T. Omura, R. Sato, *J. Biol. Chem.* **1964**, *239*, 2379–2385.

[46] O. H. Lowry, N. J. Rosebrough, A. L. Farr, R. J. Randall, *J. Biol. Chem.* **1951**, *193*, 265–275.

Supporting Information

Content: ^{1}H and ^{13}C NMR spectra of **CP1**, **CP2**, **CP3a**, **CP3b**, and **DesMeFC3**; crystal structure data of **PA1**.

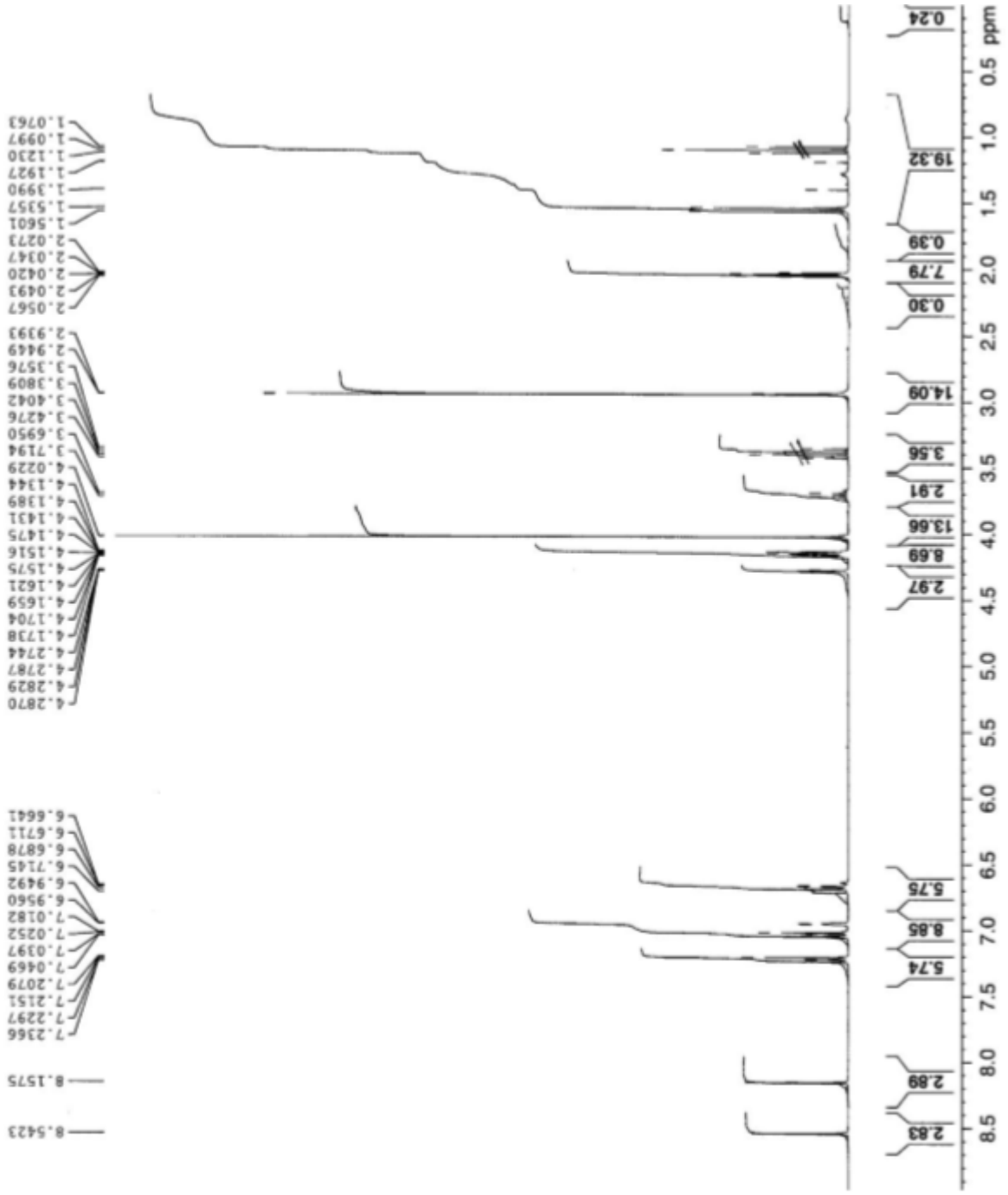

Figure S1. ^{1}H NMR Spectrum of CP1

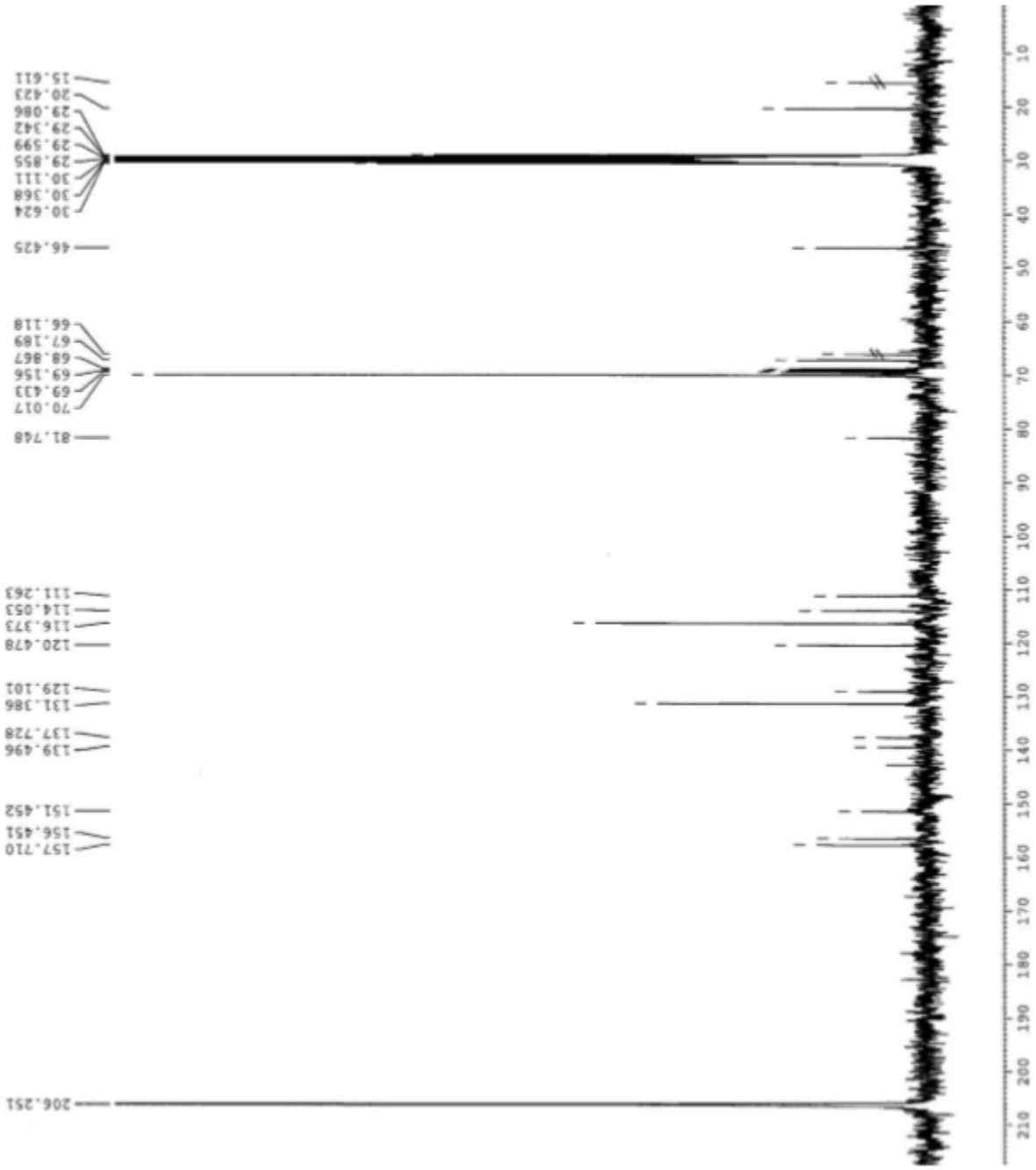

Figure S2. ^{13}C NMR Spectrum of CP1

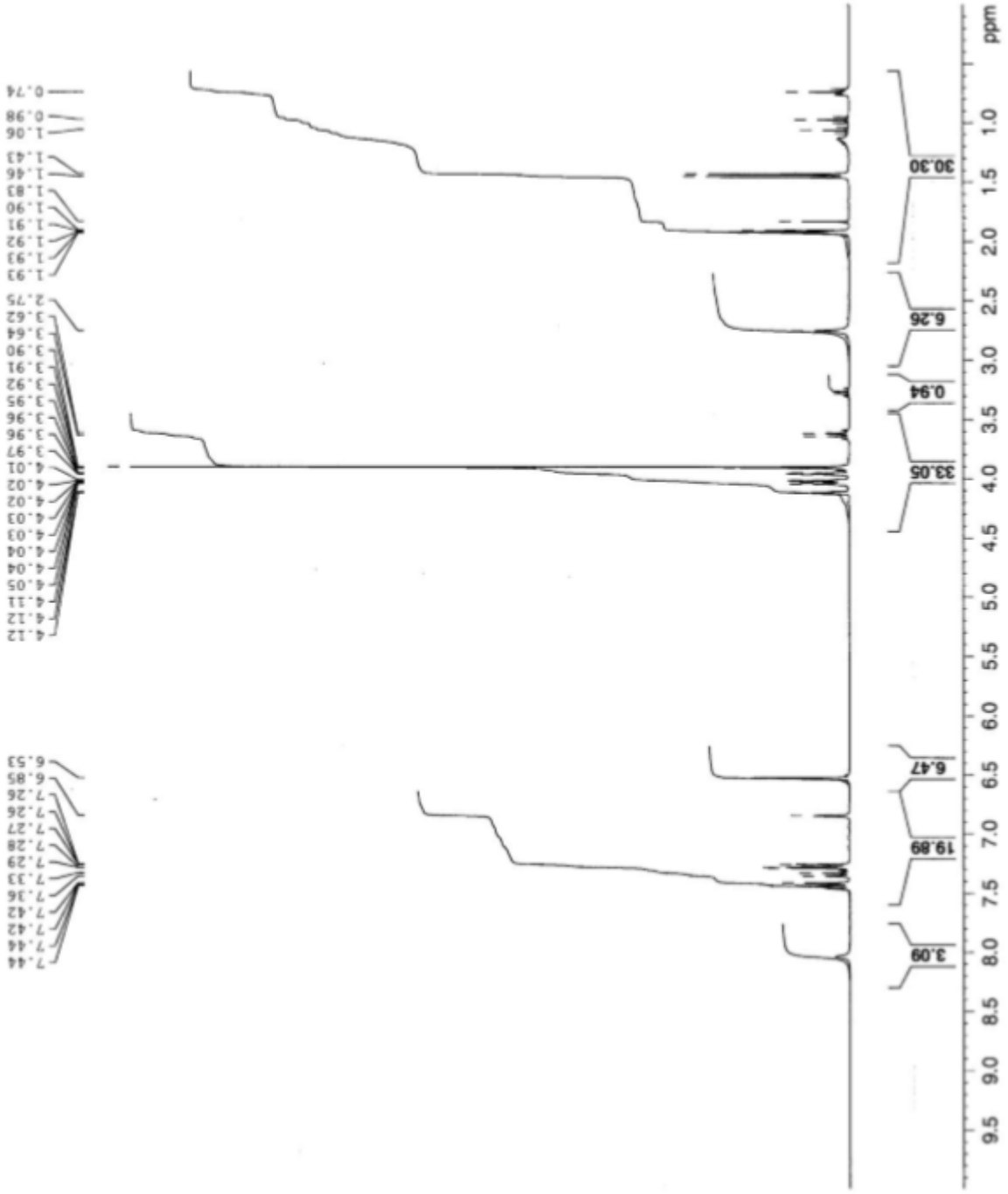

Figure S3. ^{1}H NMR Spectrum of CP2

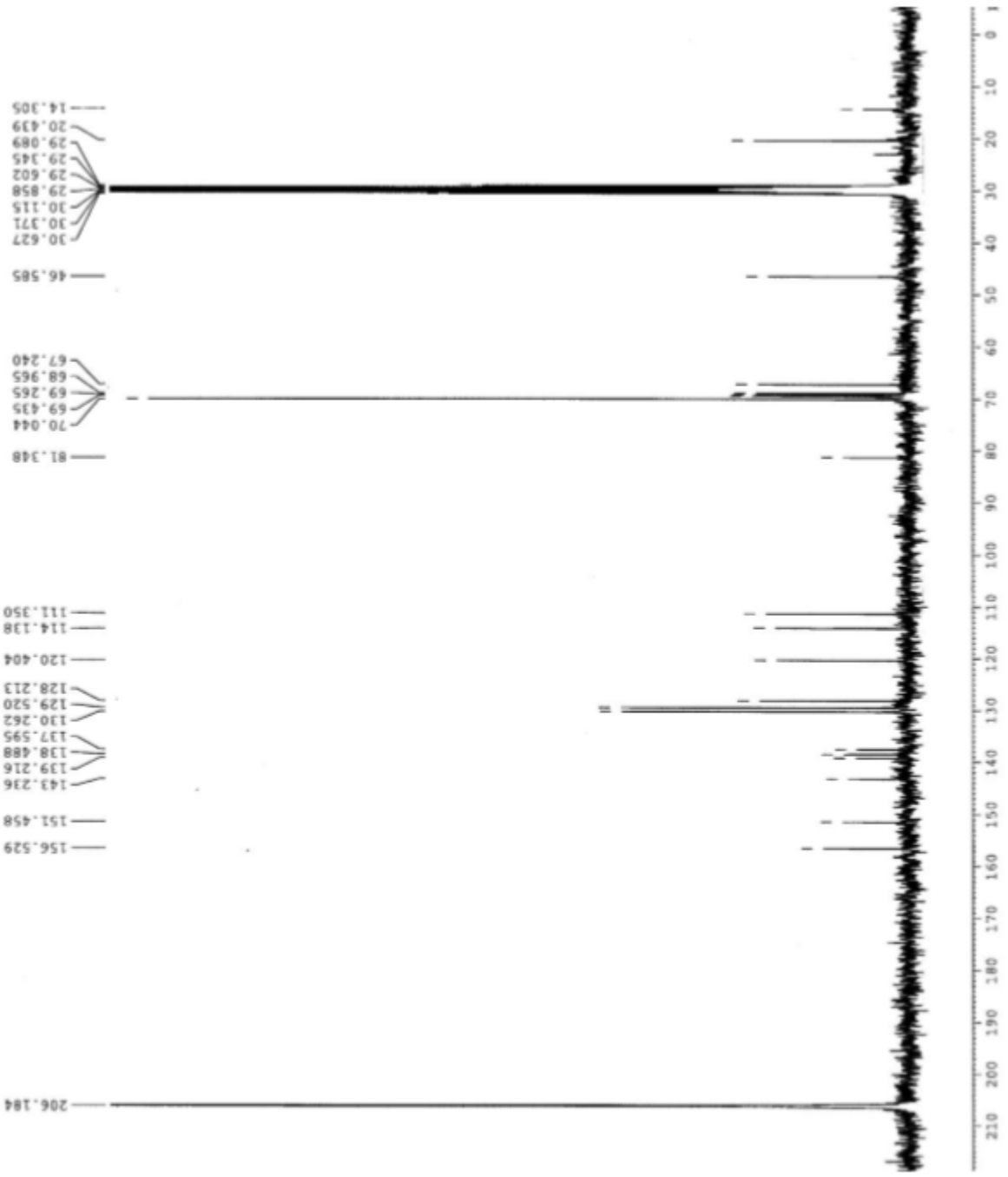

Figure S4. ^{13}C NMR Spectrum of CP2

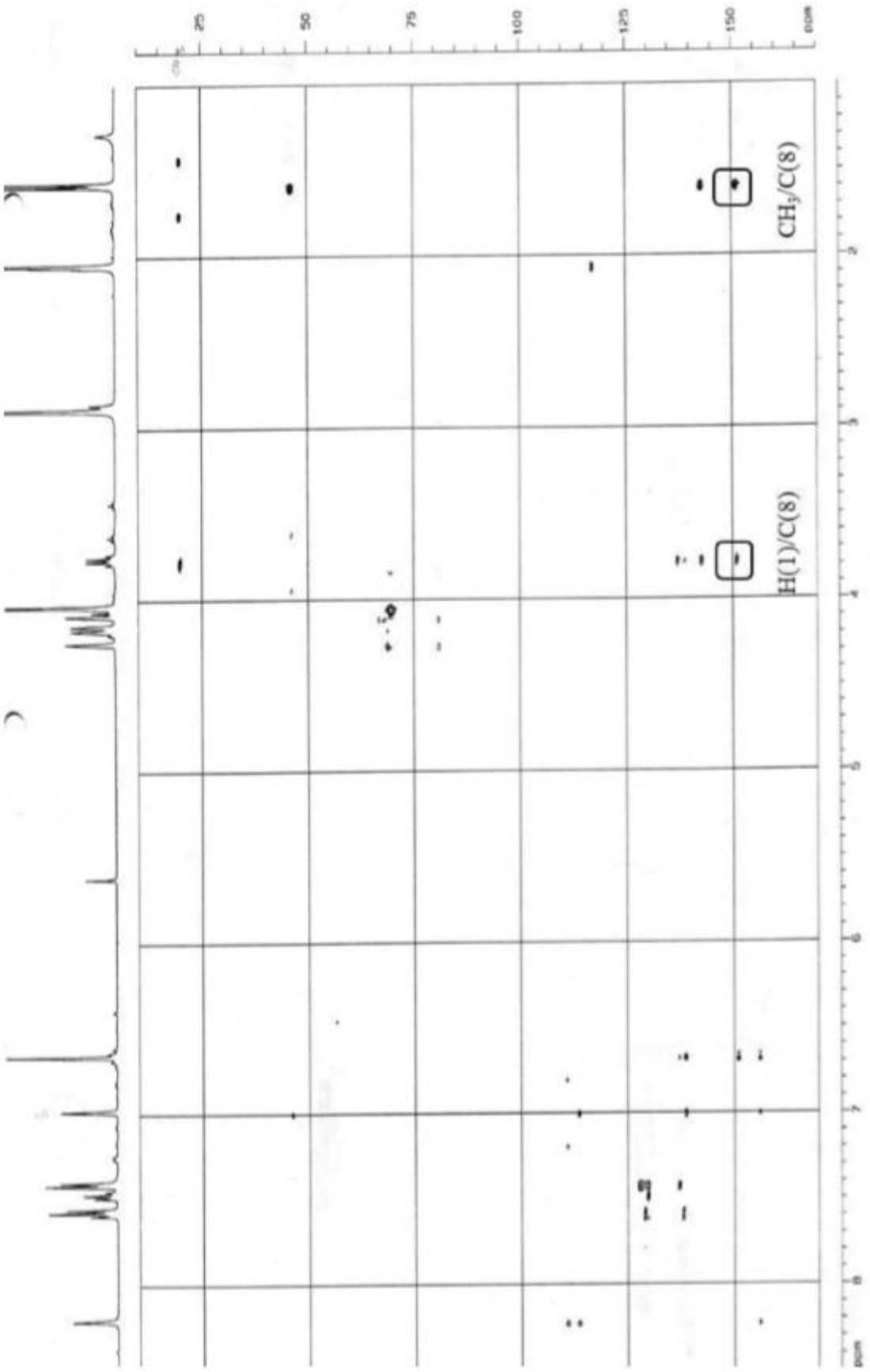

Figure S5. HMBC Spectrum of CP2

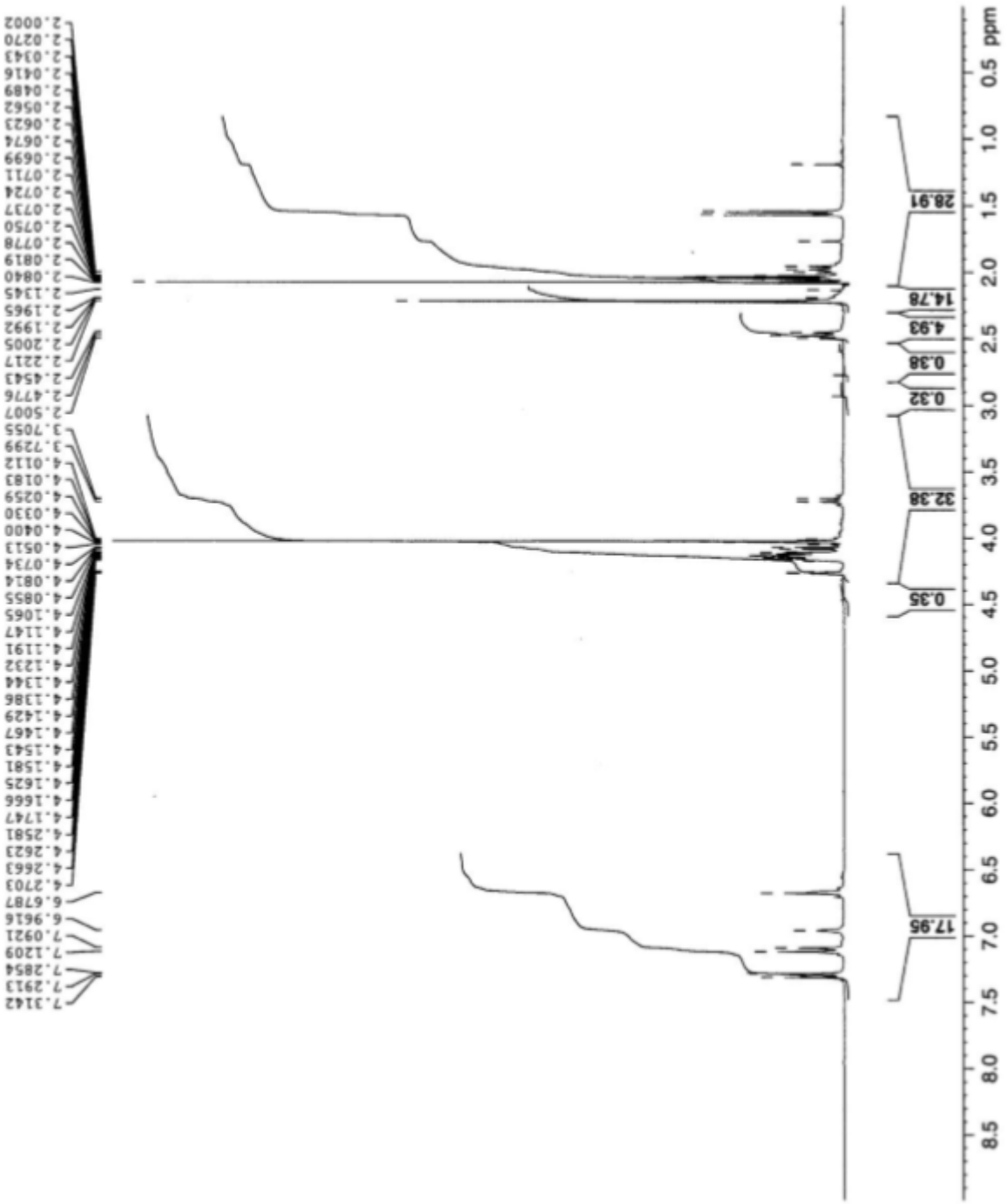

Figure S6. ^{1}H NMR Spectrum of CP3a

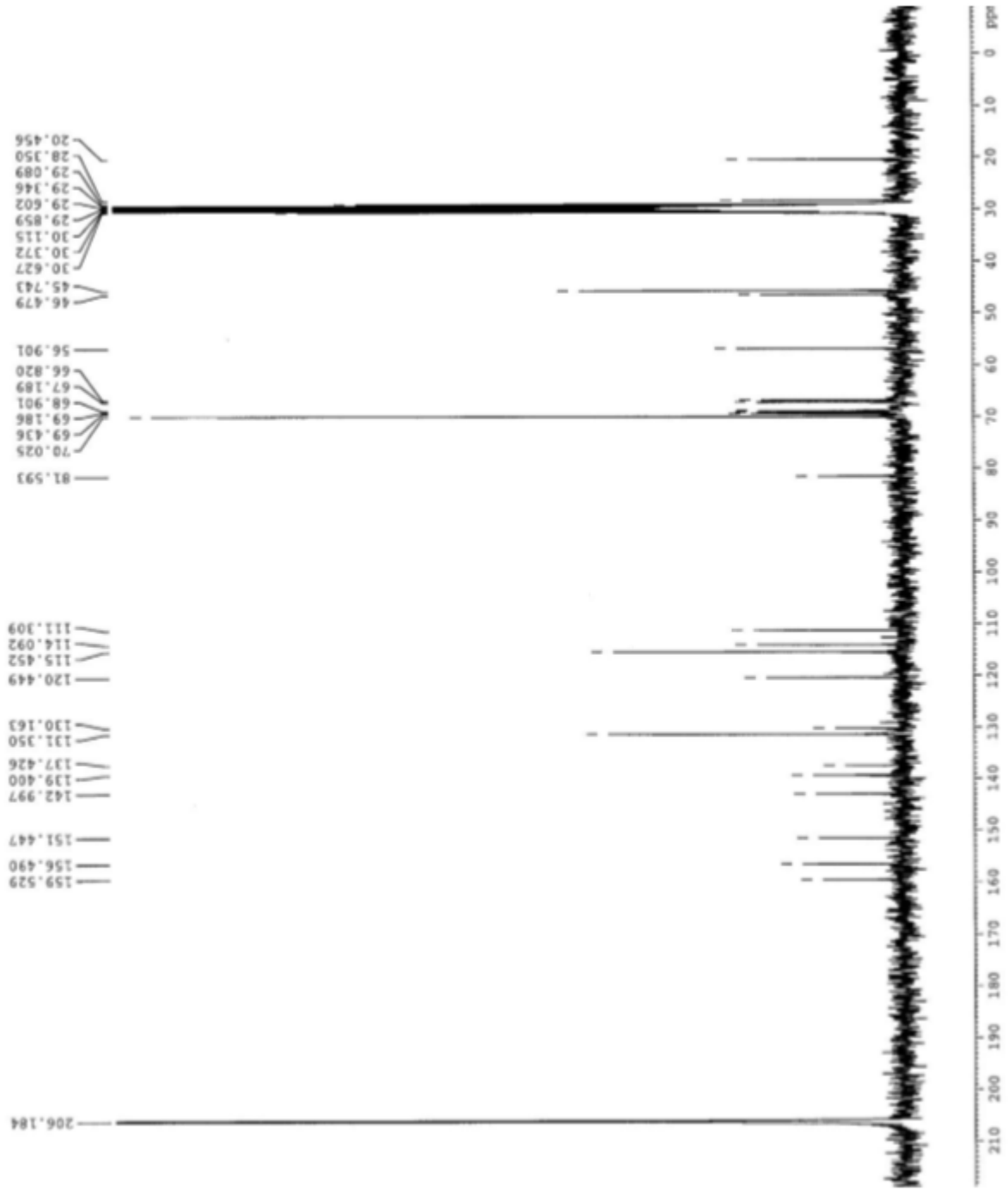

Figure S7. ^{13}C NMR Spectrum of CP3a

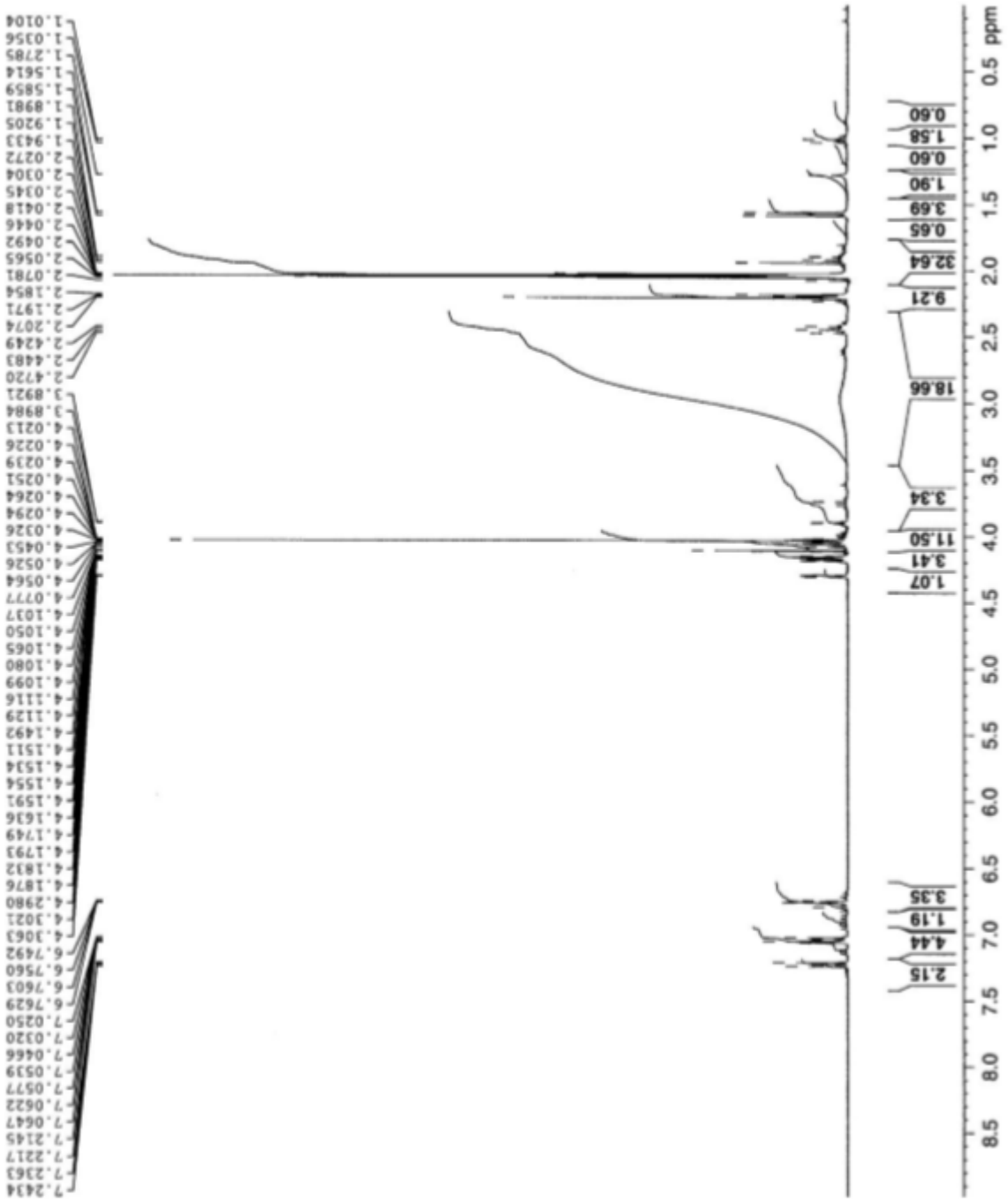

Figure S8. ^{1}H NMR Spectrum of CP3b

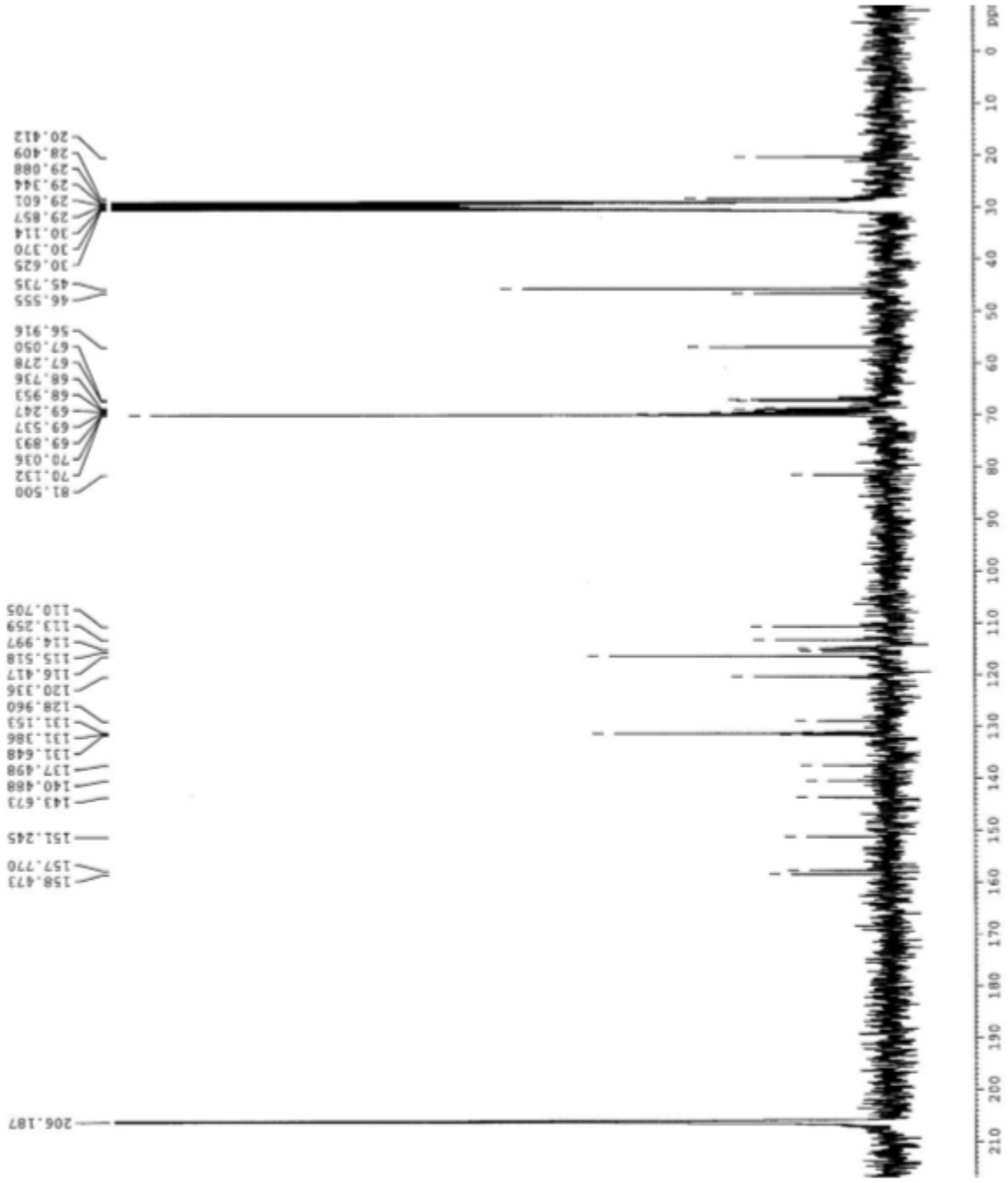

Figure S9. ^{13}C NMR Spectrum of CP3b

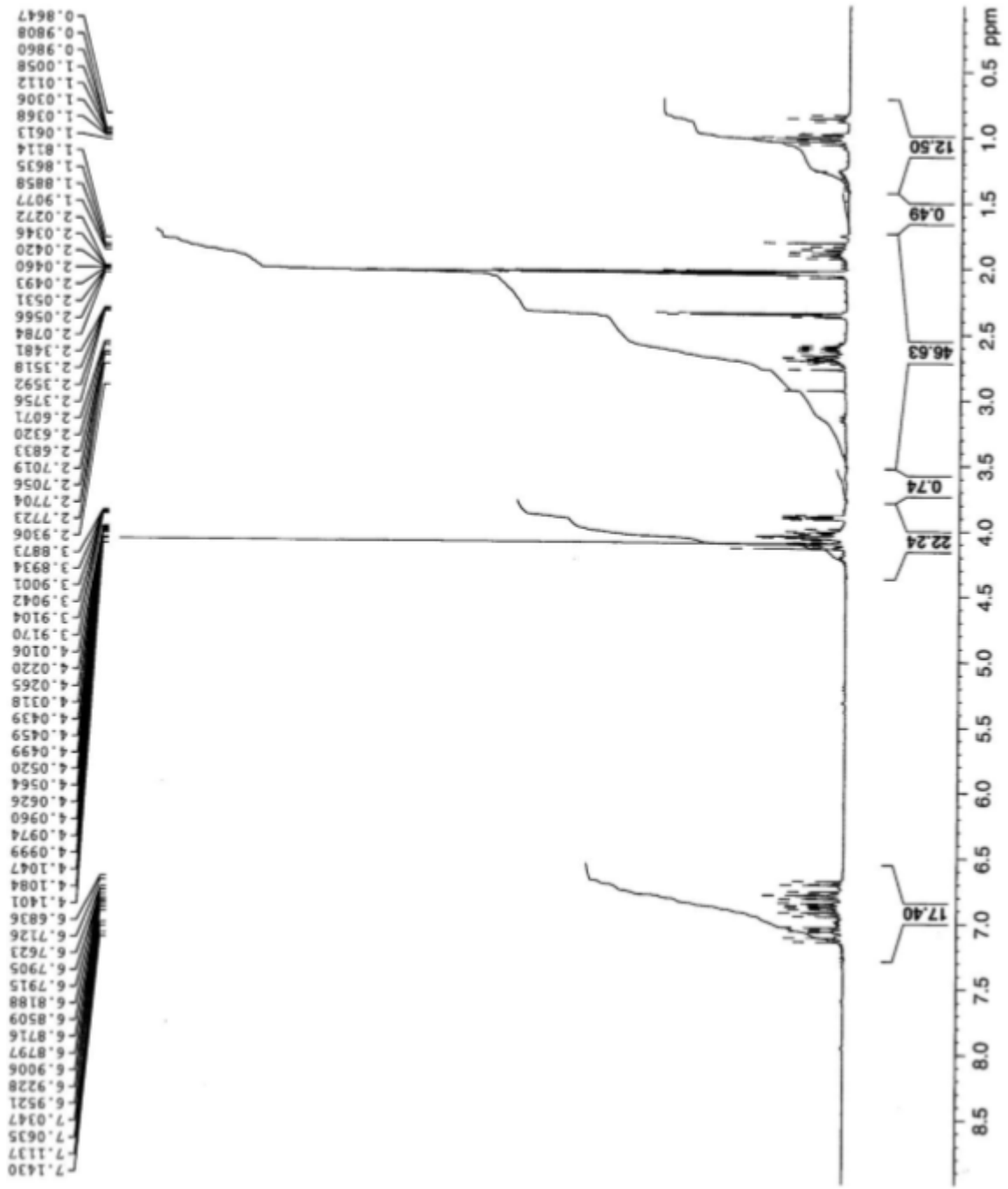

Figure S10. ^{1}H NMR Spectrum of DesMeFC3

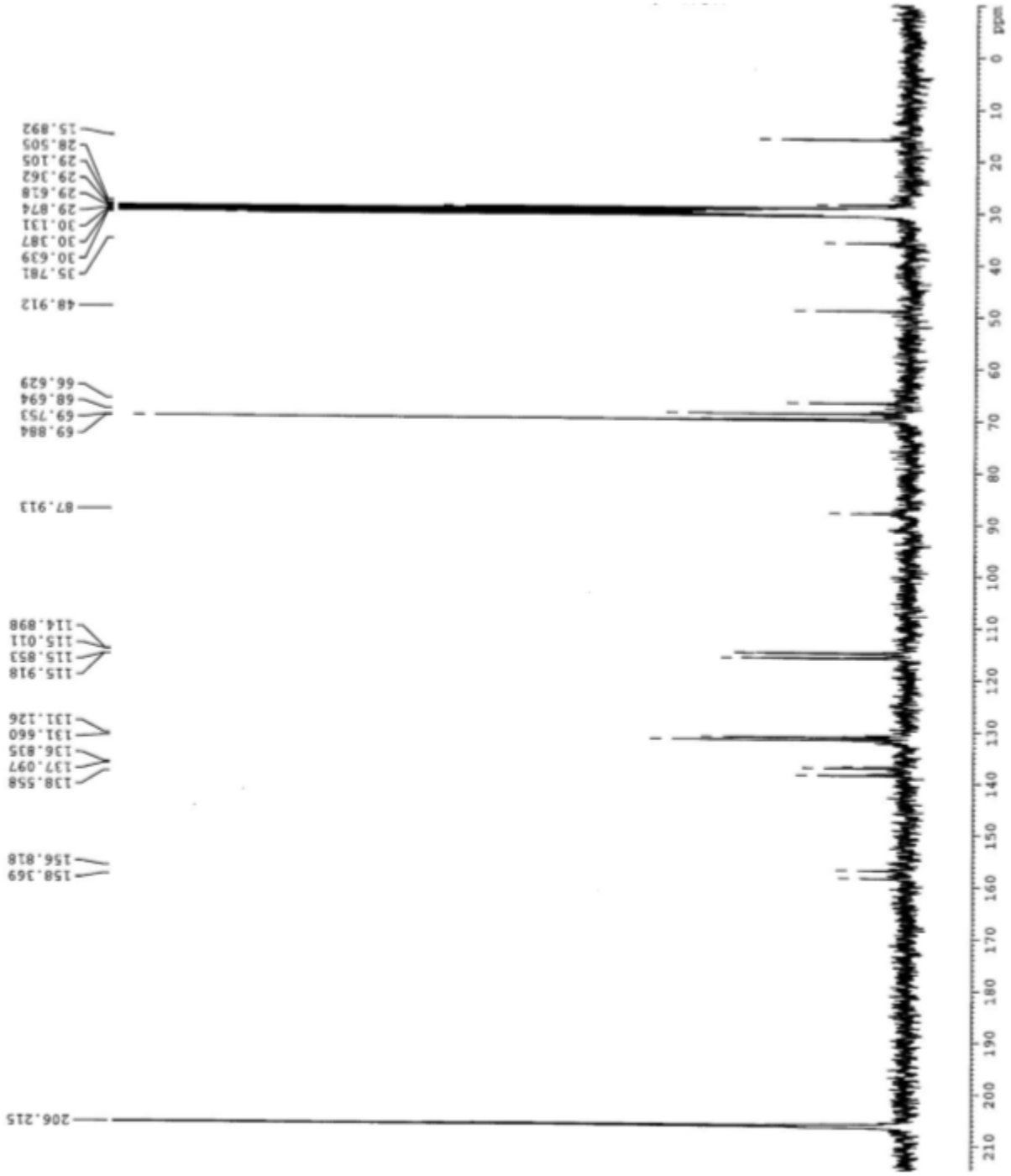

Figure S11. ^{13}C NMR Spectrum of DesMeFC3

Crystal structure information Of PA1

==========

Formula	**C26H24FeO3**		
Crystal Class	**monoclinic**	**Space Group**	**P 21/c**
A	**9.9877(4)**	**alpha**	**90**
B	**20.7297(8)**	**beta**	**108.5540(10)**
C	**10.6135(4)**	**gamma**	**90**
Volume	**2083.23(14)**	**Z**	**4**
Radiation type	**Mo Kα**	**Wavelength**	**0.710730**
P	**1.40**	**Mr**	**440.32**
M	**0.749**	**Temperature (K)**	**200(2)**
Size	**0.06x 0.08x 0.11**		
Colour	**orange**	**Shape**	**bloc**
Cell from	**9821 Reflections**	**Theta range**	**2 to 30**
Diffractometer type	**APEX2**	**Scan type**	**PHI-OMEGA**
Absorption type	**multi-scan**	**Transmission range**	**0.94 0.96**
Reflections measured	**32389**	**Independent reflections**	**6375**
Rint	**0.04**	**Theta max**	**30.54**
Hmin, Hmax	**-14 13**		
Kmin, Kmax	**-26 29**		
Lmin, Lmax	**-12 15**		
Refinement on Fsqd			
R[I>2σ(I)]	**0.030**	**WR2(all)**	**0.062**
		Max shift/su	**0.0015**
Delta Rho min	**-0.49**	**Delta Rho max**	**0.49**
Reflections used	**6358**		
Number of parameters	**272**	**Goodness of fit**	**0.995**

Table S1 : Fractional atomic coordinates for C26H24FeO3

Atom	x/a	y/b	z/c	U(eqv)
Fe(1)	0.727401(18)	0.346740(8)	0.493695(19)	0.0239
C(1)	0.78376(16)	0.43963(7)	0.55010(15)	0.0367
C(2)	0.67330(16)	0.41940(7)	0.59861(15)	0.0347
C(3)	0.72108(16)	0.36459(8)	0.68151(15)	0.0370
C(4)	0.86147(16)	0.35127(8)	0.68472(16)	0.0405
C(5)	0.90017(15)	0.39761(8)	0.60344(16)	0.0403
C(9)	0.55595(12)	0.32474(5)	0.33084(12)	0.0204
C(10)	0.67643(13)	0.34228(6)	0.29203(14)	0.0273
C(11)	0.78834(14)	0.29846(7)	0.35376(17)	0.0370
C(12)	0.73963(15)	0.25464(7)	0.43162(17)	0.0362
C(13)	0.59700(13)	0.27034(6)	0.41826(14)	0.0270
C(14)	0.41815(11)	0.35813(5)	0.28895(11)	0.0190
C(15)	0.42309(12)	0.43085(5)	0.27385(12)	0.0221
C(16)	0.39495(16)	0.44944(6)	0.12966(14)	0.0323
C(18)	0.29393(11)	0.32581(5)	0.25730(11)	0.0186
C(19)	0.15609(11)	0.36083(5)	0.22427(11)	0.0195
C(20)	0.06044(13)	0.35933(6)	0.09571(12)	0.0246
C(21)	-0.06279(13)	0.39589(6)	0.06002(12)	0.0251
C(22)	-0.09365(12)	0.43311(5)	0.15581(12)	0.0221
C(24)	-0.00348(14)	0.43337(7)	0.28554(13)	0.0278
C(25)	0.12060(13)	0.39765(6)	0.31876(12)	0.0259
C(26)	0.28862(11)	0.25425(5)	0.24497(11)	0.0183
C(27)	0.35406(13)	0.22346(6)	0.16322(12)	0.0224
C(28)	0.35920(13)	0.15680(6)	0.15593(13)	0.0241
C(29)	0.29957(12)	0.11949(5)	0.23246(13)	0.0229
C(31)	0.22921(13)	0.14877(6)	0.31121(13)	0.0233
C(32)	0.22315(12)	0.21584(6)	0.31591(12)	0.0216
O(17)	0.39490(11)	0.51813(5)	0.11231(11)	0.0357
O(23)	-0.21400(10)	0.46999(5)	0.12782(10)	0.0322
O(30)	0.31416(11)	0.05362(4)	0.22653(12)	0.0342

Table S2 : Interatomic distances (Å) for C26H24FeO3

Fe(1)	- C(2)	2.0454(15)	Fe(1)	- C(3)	2.0480(16)
Fe(1)	- C(4)	2.0457(15)	Fe(1)	- C(5)	2.0414(14)
Fe(1)	- C(9)	2.0601(11)	Fe(1)	- C(10)	2.0385(14)
Fe(1)	- C(11)	2.0380(15)	Fe(1)	- C(12)	2.0361(14)
Fe(1)	- C(13)	2.0450(12)	Fe(1)	- C(1)	2.0416(14)
C(2)	- C(3)	1.423(2)	C(2)	- C(1)	1.421(2)
C(3)	- C(4)	1.419(2)	C(4)	- C(5)	1.424(2)
C(5)	- C(1)	1.418(2)	C(9)	- C(10)	1.4371(17)
C(9)	- C(13)	1.4348(16)	C(9)	- C(14)	1.4771(15)
C(10)	- C(11)	1.4276(19)	C(11)	- C(12)	1.414(2)
C(12)	- C(13)	1.4237(18)	C(14)	- C(15)	1.5184(15)
C(14)	- C(18)	1.3550(15)	C(15)	- C(16)	1.5151(18)
C(16)	- O(17)	1.4358(15)	C(18)	- C(19)	1.4961(15)
C(18)	- C(26)	1.4885(15)	C(19)	- C(20)	1.3949(16)
C(19)	- C(25)	1.3930(16)	C(20)	- C(21)	1.3915(16)
C(21)	- C(22)	1.3867(17)	C(22)	- C(24)	1.3848(17)
C(22)	- O(23)	1.3749(14)	C(24)	- C(25)	1.3893(17)
C(26)	- C(27)	1.3959(16)	C(26)	- C(32)	1.3934(16)
C(27)	- C(28)	1.3860(16)	C(28)	- C(29)	1.3857(17)
C(29)	- C(31)	1.3908(17)	C(29)	- O(30)	1.3769(14)
C(31)	- C(32)	1.3934(16)			

Table S3 :Bond angles (°) for C26H24FeO3

C(2)	- Fe(1)	- C(3)	40.70(6)	C(2)	- Fe(1)	- C(4)	68.26(7)
C(3)	- Fe(1)	- C(4)	40.56(6)	C(2)	- Fe(1)	- C(5)	68.33(7)
C(3)	- Fe(1)	- C(5)	68.51(7)	C(4)	- Fe(1)	- C(5)	40.79(6)
C(2)	- Fe(1)	- C(9)	109.07(5)	C(3)	- Fe(1)	- C(9)	125.58(5)

C(4)	- Fe(1)	- C(9)	161.60(6)	C(5)	- Fe(1)	- C(9)	156.80(6)
C(2)	- Fe(1)	- C(10)	125.73(6)	C(3)	- Fe(1)	- C(10)	162.82(6)
C(4)	- Fe(1)	- C(10)	155.33(6)	C(5)	- Fe(1)	- C(10)	120.39(6)
C(9)	- Fe(1)	- C(10)	41.05(5)	C(2)	- Fe(1)	- C(11)	161.86(7)
C(3)	- Fe(1)	- C(11)	155.08(7)	C(4)	- Fe(1)	- C(11)	119.45(7)
C(5)	- Fe(1)	- C(11)	105.98(7)	C(9)	- Fe(1)	- C(11)	68.97(5)
C(2)	- Fe(1)	- C(12)	156.95(7)	C(3)	- Fe(1)	- C(12)	120.53(7)
C(4)	- Fe(1)	- C(12)	106.02(7)	C(5)	- Fe(1)	- C(12)	122.83(6)
C(9)	- Fe(1)	- C(12)	68.92(5)	C(2)	- Fe(1)	- C(13)	122.53(6)
C(3)	- Fe(1)	- C(13)	107.93(6)	C(4)	- Fe(1)	- C(13)	123.92(6)
C(5)	- Fe(1)	- C(13)	160.20(6)	C(9)	- Fe(1)	- C(13)	40.91(5)
C(2)	- Fe(1)	- C(1)	40.69(6)	C(3)	- Fe(1)	- C(1)	68.61(7)
C(4)	- Fe(1)	- C(1)	68.51(6)	C(5)	- Fe(1)	- C(1)	40.66(6)
C(9)	- Fe(1)	- C(1)	122.20(5)	C(10)	- Fe(1)	- C(11)	41.00(6)
C(10)	- Fe(1)	- C(12)	68.80(6)	C(11)	- Fe(1)	- C(12)	40.63(7)
C(10)	- Fe(1)	- C(13)	68.82(5)	C(11)	- Fe(1)	- C(13)	68.59(6)
C(12)	- Fe(1)	- C(13)	40.83(5)	C(10)	- Fe(1)	- C(1)	107.70(6)
C(11)	- Fe(1)	- C(1)	123.95(7)	C(12)	- Fe(1)	- C(1)	160.04(6)
C(13)	- Fe(1)	- C(1)	157.98(6)	Fe(1)	- C(2)	- C(3)	69.75(9)
Fe(1)	- C(2)	- C(1)	69.51(9)	C(3)	- C(2)	- C(1)	108.25(13)
Fe(1)	- C(3)	- C(2)	69.55(8)	Fe(1)	- C(3)	- C(4)	69.63(9)
C(2)	- C(3)	- C(4)	107.73(14)	Fe(1)	- C(4)	- C(3)	69.81(8)
Fe(1)	- C(4)	- C(5)	69.45(8)	C(3)	- C(4)	- C(5)	108.11(14)
Fe(1)	- C(5)	- C(4)	69.77(8)	Fe(1)	- C(5)	- C(1)	69.68(8)
C(4)	- C(5)	- C(1)	108.05(14)	Fe(1)	- C(9)	- C(10)	68.67(7)
Fe(1)	- C(9)	- C(13)	68.98(7)	C(10)	- C(9)	- C(13)	106.93(10)
Fe(1)	- C(9)	- C(14)	126.51(8)	C(10)	- C(9)	- C(14)	125.45(11)
C(13)	- C(9)	- C(14)	127.60(11)	Fe(1)	- C(10)	- C(9)	70.28(7)
Fe(1)	- C(10)	- C(11)	69.48(9)	C(9)	- C(10)	- C(11)	108.19(12)

Fe(1)	- C(11)	- C(10)	69.52(8)	Fe(1)	- C(11)	- C(12)	69.61(9)
C(10)	- C(11)	- C(12)	108.19(12)	Fe(1)	- C(12)	- C(11)	69.76(8)
Fe(1)	- C(12)	- C(13)	69.92(7)	C(11)	- C(12)	- C(13)	108.32(12)
Fe(1)	- C(13)	- C(9)	70.11(7)	Fe(1)	- C(13)	- C(12)	69.25(7)
C(9)	- C(13)	- C(12)	108.36(12)	C(9)	- C(14)	- C(15)	116.02(10)
C(9)	- C(14)	- C(18)	122.33(10)	C(15)	- C(14)	- C(18)	121.52(10)
C(14)	- C(15)	- C(16)	110.94(10)	C(15)	- C(16)	- O(17)	111.98(11)
C(14)	- C(18)	- C(19)	121.32(10)	C(14)	- C(18)	- C(26)	121.26(10)
C(19)	- C(18)	- C(26)	117.30(9)	C(18)	- C(19)	- C(20)	120.74(10)
C(18)	- C(19)	- C(25)	121.55(10)	C(20)	- C(19)	- C(25)	117.68(10)
C(19)	- C(20)	- C(21)	121.68(11)	C(20)	- C(21)	- C(22)	119.15(11)
C(21)	- C(22)	- C(24)	120.34(11)	C(21)	- C(22)	- O(23)	122.27(11)
C(24)	- C(22)	- O(23)	117.38(11)	C(22)	- C(24)	- C(25)	119.71(11)
C(19)	- C(25)	- C(24)	121.34(11)	C(18)	- C(26)	- C(27)	119.98(10)
C(18)	- C(26)	- C(32)	122.12(10)	C(27)	- C(26)	- C(32)	117.88(10)
C(26)	- C(27)	- C(28)	121.57(11)	C(27)	- C(28)	- C(29)	119.55(11)
C(28)	- C(29)	- C(31)	120.16(11)	C(28)	- C(29)	- O(30)	117.08(11)
C(31)	- C(29)	- O(30)	122.77(11)	C(29)	- C(31)	- C(32)	119.53(11)
C(26)	- C(32)	- C(31)	121.18(11)	Fe(1)	- C(1)	- C(2)	69.80(8)
Fe(1)	- C(1)	- C(5)	69.66(8)	C(2)	- C(1)	- C(5)	107.85(14)

Table S4 : Anisotropic thermal parameters for C26H24FeO3

Atom	u(11)	u(22)	u(33)	u(23)	u(13)	u(12)
Fe(1)	0.01606(8)	0.02056(8)	0.03032(10)	0.00099(6)	0.00059(7)	-0.00018(6)
C(1)	0.0375(7)	0.0273(6)	0.0376(7)	-0.0037(5)	0.0010(6)	-0.0104(6)
C(2)	0.0359(7)	0.0305(6)	0.0329(7)	-0.0094(5)	0.0043(6)	-0.0024(5)
C(3)	0.0347(7)	0.0422(8)	0.0289(6)	0.0005(6)	0.0029(5)	-0.0063(6)
C(4)	0.0274(7)	0.0460(9)	0.0361(7)	0.0072(6)	-0.0066(6)	-0.0041(6)
C(5)	0.0250(6)	0.0451(8)	0.0415(8)	0.0011(7)	-0.0026(6)	-0.0124(6)

C(9)	0.0168(5)	0.0163(5)	0.0261(5)	-0.0009(4)	0.0040(4)	-0.0001(4)
C(10)	0.0213(5)	0.0288(6)	0.0331(6)	-0.0032(5)	0.0103(5)	-0.0019(4)
C(11)	0.0209(6)	0.0357(7)	0.0544(9)	-0.0105(6)	0.0118(6)	0.0040(5)
C(12)	0.0247(6)	0.0213(6)	0.0543(9)	-0.0021(6)	0.0011(6)	0.0067(5)
C(13)	0.0224(5)	0.0168(5)	0.0369(6)	0.0025(4)	0.0023(5)	0.0000(4)
C(14)	0.0175(5)	0.0151(4)	0.0223(5)	0.0011(4)	0.0036(4)	0.0008(4)
C(15)	0.0205(5)	0.0151(5)	0.0278(5)	0.0012(4)	0.0034(4)	-0.0014(4)
C(16)	0.0406(7)	0.0192(5)	0.0302(6)	0.0054(5)	0.0014(5)	-0.0048(5)
C(18)	0.0169(4)	0.0153(4)	0.0227(5)	0.0005(4)	0.0048(4)	0.0010(4)
C(19)	0.0154(4)	0.0161(4)	0.0254(5)	0.0010(4)	0.0041(4)	0.0000(4)
C(20)	0.0212(5)	0.0247(5)	0.0254(5)	-0.0051(4)	0.0039(4)	0.0017(4)
C(21)	0.0207(5)	0.0263(6)	0.0238(5)	0.0000(4)	0.0006(4)	0.0018(4)
C(22)	0.0176(5)	0.0177(5)	0.0287(6)	0.0027(4)	0.0040(4)	0.0028(4)
C(24)	0.0245(5)	0.0309(6)	0.0262(6)	-0.0042(5)	0.0058(5)	0.0071(5)
C(25)	0.0207(5)	0.0306(6)	0.0229(5)	-0.0016(4)	0.0021(4)	0.0050(4)
C(26)	0.0155(4)	0.0155(4)	0.0221(5)	-0.0002(4)	0.0032(4)	-0.0004(3)
C(27)	0.0229(5)	0.0206(5)	0.0250(5)	-0.0013(4)	0.0095(4)	-0.0027(4)
C(28)	0.0230(5)	0.0213(5)	0.0290(6)	-0.0066(4)	0.0096(5)	-0.0017(4)
C(29)	0.0183(5)	0.0154(5)	0.0319(6)	-0.0021(4)	0.0036(4)	-0.0008(4)
C(31)	0.0213(5)	0.0182(5)	0.0311(6)	0.0021(4)	0.0093(4)	-0.0019(4)
C(32)	0.0199(5)	0.0186(5)	0.0278(5)	-0.0006(4)	0.0097(4)	-0.0001(4)
O(17)	0.0336(5)	0.0213(4)	0.0409(5)	0.0111(4)	-0.0040(4)	-0.0056(4)
O(23)	0.0243(4)	0.0309(5)	0.0353(5)	0.0009(4)	0.0006(4)	0.0128(4)
O(30)	0.0345(5)	0.0151(4)	0.0556(6)	-0.0029(4)	0.0180(5)	-0.0004(4)

Table S5 : Hydrogen atoms fractional atomic coordinates for C26H24FeO3

Atom	x/a	y/b	z/c	U(iso)
H(1)	0.4746	0.5314	0.1546	0.0396(10)
H(11)	0.7801	0.4754	0.4918	0.0396(10)
H(2)	0.2724	0.0360	0.2734	0.0396(10)
H(3)	-0.2642	0.4669	0.0542	0.0396(10)
H(21)	0.5815	0.4388	0.5775	0.0396(10)
H(31)	0.6673	0.3409	0.7270	0.0396(10)
H(41)	0.9195	0.3168	0.7323	0.0396(10)
H(51)	0.9889	0.3999	0.5874	0.0396(10)
H(101)	0.6808	0.3773	0.2343	0.0396(10)
H(111)	0.8805	0.2990	0.3449	0.0396(10)
H(121)	0.7936	0.2205	0.4846	0.0396(10)
H(131)	0.5385	0.2488	0.4609	0.0396(10)
H(151)	0.5140	0.4463	0.3254	0.0396(10)
H(152)	0.3535	0.4504	0.3057	0.0396(10)
H(161)	0.4661	0.4305	0.0981	0.0396(10)
H(162)	0.3052	0.4328	0.0774	0.0396(10)
H(201)	0.0802	0.3325	0.0307	0.0396(10)
H(211)	-0.1250	0.3958	-0.0294	0.0396(10)
H(241)	-0.0268	0.4583	0.3516	0.0396(10)
H(251)	0.1833	0.3984	0.4082	0.0396(10)
H(271)	0.3956	0.2489	0.1107	0.0396(10)
H(281)	0.4038	0.1365	0.0989	0.0396(10)
H(311)	0.1854	0.1228	0.3611	0.0396(10)
H(321)	0.1726	0.2358	0.3683	0.0396(10)